ACS Infectious Diseases

pubs.acs.org/journal/aidcbc

Article

A Recombinant Subunit Vaccine Induces a Potent, Broadly Neutralizing, and Durable Antibody Response in Macaques against the SARS-CoV-2 P.1 (Gamma) Variant

Albert To, Teri Ann S. Wong, Michael M. Lieberman, Karen Thompson, Aquena H. Ball, Laurent Pessaint, Jack Greenhouse, Nisrine Daham, Anthony Cook, Brandon Narvaez, Zack Flinchbaugh, Alex Van Ry, Jake Yalley-Ogunro, Hanne Andersen Elyard, Chih-Yun Lai, Oreola Donini, and Axel T. Lehrer*

Cite This: https://doi.org/10.1021/acsinfecdis.1c00600

Read Online

ACCESS | Metrics & More | Article Recommendations | Supporting Information

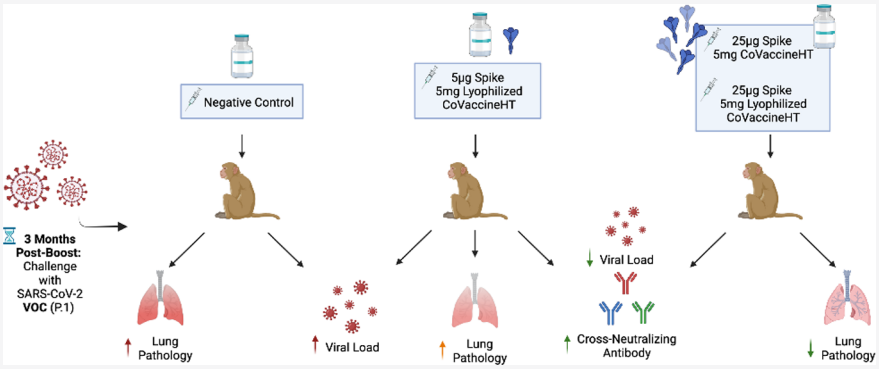

ABSTRACT: FDA-approved and emergency use-authorized vaccines using new mRNA and viral-vector technology are highly effective in preventing moderate to severe disease; however, information on their long-term efficacy and protective breadth against severe acute respiratory syndrome coronavirus 2 variants of concern (VOCs) is currently scarce. Here, we describe the durability and broad-spectrum VOC immunity of a prefusion-stabilized spike (S) protein adjuvanted with liquid or lyophilized CoVaccine HT in cynomolgus macaques. This recombinant subunit vaccine is highly immunogenic and induces robust spike-specific and broadly neutralizing antibody responses effective against circulating VOCs (B.1.351 [Beta], P.1 [Gamma], and B.1.617 [Delta]) for at least three months after the final boost. Protective efficacy and postexposure immunity were evaluated using a heterologous P.1 challenge nearly three months after the last immunization. Our results indicate that while immunization with both high and low S doses shorten and reduce viral loads in the upper and lower respiratory tract, a higher antigen dose is required to provide durable protection against disease as vaccine immunity wanes. Histologically, P.1 infection causes similar COVID-19-like lung pathology as seen with early pandemic isolates. Postchallenge IgG concentrations were restored to peak immunity levels, and vaccine-matched and cross-variant neutralizing antibodies were significantly elevated in immunized macaques indicating an efficient anamnestic response. Only low levels of P.1-specific neutralizing antibodies with limited breadth were observed in control (nonvaccinated but challenged) macaques, suggesting that natural infection may not prevent reinfection by other VOCs. Overall, these results demonstrate that a properly dosed and adjuvanted recombinant subunit vaccine can provide protective immunity against circulating VOCs for at least three months.

KEYWORDS: *SARS-CoV-2, subunit protein vaccine, lyophilized, CoVaccine HT, cynomolgus macaques, delayed challenge*

COVID-19 is a respiratory disease caused by the severe acute respiratory syndrome coronavirus 2 (SARS-CoV-2)[1,2] and is commonly characterized as an asymptomatic infection or a self-limiting, febrile illness copresented with cough, shortness of breath, and fatigue.[3,4] Severe complications can result in approximately 6−10% of infected patients[5] developing pneumonia, acute respiratory distress syndrome, multiorgan dysfunction, and arterial thromboembolic events

Received: November 10, 2021

that can result in hospitalization and/or death.[6−9] Transmission occurs through respiratory droplets during close contact with asymptomatic or presymptomatic infected individuals, as well as symptomatic patients.[10−12] The synergistic relationship between infectivity and high transmissibility with low virulence has contributed to the ongoing global public health crisis and the emergence of more transmissible and potentially more pathogenic variants of concern (VOCs). Longitudinal cross-sectional studies have indicated that only a fraction of asymptomatic to mild and moderate SARS-CoV-2 natural infections of humans results in detectable neutralizing antibodies months after recovery,[13−15] and current evidence suggests that convalescent immunity may only provide transient protection.[16−18] Furthermore, the degree of immune evasion witnessed in vitro by spike (S) protein variants and the increasing occurrence of reinfection[19−23] have raised the question whether previous infection or vaccine-derived immunity can provide heterologous protection against further transmission and limit additional mutation of circulating VOCs, even while protection against severe disease and mortality has been sustained to date.

Some VOCs show increased transmissibility, cause more severe disease than original strains, and demonstrate greater immune evasion to neutralizing antibodies as they harbor mutations at sites facilitating viral fusion and at critical epitopes in the N-terminal (NTD) and receptor-binding domains (RBD).[24,25] The B.1.1.7 (Alpha), B.1.351 (Beta), and P.1 (Gamma) variants contain the same set of mutations, K417T, E484K, and N501Y, while the B.1.617 (Delta) carries L452R and T478K mutations, all of which are associated with enhanced infectivity and reduced serum neutralization.[26−28] These antigenic changes have abolished potent neutralizing epitopes targeted by monoclonal antibody therapeutics[29] and antibodies elicited by mRNA vaccination.[30] Natural reinfection with the VOC strains after the original strain infection, and vice versa, has been documented.[20,31−34] Despite this, cross-neutralization of convalescent sera from patients infected with nonvariants and mRNA-immunized individuals suggests that the parental spike (S) protein in current vaccines affords some degree of protection.[35−37]

Phase 1−3 clinical trials of novel mRNA (Moderna mRNA-1273 and Pfizer-BioNTech BNT162b2) and viral-vector (Johnson & Johnson−Janssen Ad26.COV2.S) platforms, utilizing the original Wuhan-Hu-1 S protein,[38−40] have shown these vaccines to be highly protective with 94−95 and 67% efficacy against COVID-19 disease, respectively,[41−43] and they all elicit uniformly high protection against severe disease/death (i.e., >85%). Post hoc sequencing during clinical trials of these and other vaccine platforms in variant-dominant regions has revealed a slightly lower efficacy against B.1.1.7 and B.1.351 variants, albeit usually remaining above the 50% protection threshold.[44,45] Attempts at predicting protection based on immune correlates, such as cross-neutralizing antibodies, have shown that vaccinated individuals have a 2- to 8-fold reduction in titers against current VOCs as IgG levels wane, which are nonetheless believed to confer a degree of resistance against infection.[46−49] However, these samples were taken during the peak period of the humoral response and may not be accurate predictors of protection months onward when the likelihood of infection is greater. Thus, understanding the decay in antibody responses months after the final boost is an essential endpoint in vaccine development.

Evaluating a delayed vaccine response in nonhuman primate (NHP) models can provide valuable foresight into the relationship between waning immunity and protection, especially against VOCs. In this study, we describe the immunogenicity and protective efficacy of a recombinant prefusion spike subunit (based on the reference SARS-CoV-2 strain, Wuhan-Hu-1) adjuvanted with liquid or lyophilized (dry) CoVaccine HT, a squalane-in-water nanoemulsion adjuvant containing immunostimulatory sucrose fatty acid sulfate esters,[50] in cynomolgus macaques. Both the zeta potential and emulsion droplet size of CoVaccine HT are maintained when reconstituted with distilled water.[51] Other investigators have shown that infection with SARS-CoV-2 (prototype strain) produced COVID-19-like disease in this species and reflects similar viral shedding kinetics and lung pathology to human infections.[52,53] We have previously demonstrated that our vaccine candidate elicits a broad-spectrum IgG response including high neutralizing antibody (NtAb) titers against the prototypic SARS-CoV-2 and VOCs, specifically B.1.351 and P.1, and an in vitro antigen-specific IFN-γ secreting response from immune splenocytes taken from Swiss Webster mice.[54] To elaborate on our understanding of the elicited immunological response, we assessed the vaccine efficacy using a delayed challenge scheme with the P.1 VOC to delineate how the maturation or decay of the humoral response affects protection from a heterologous SARS-CoV-2 strain. Neutralizing antibody responses to the vaccine-matched WA1/2020 strain and VOCs B.1.351, P.1, and B.1.617 were also determined just prior to challenge and 14 days postchallenge (to assess anamnestic responses). Furthermore, we characterize the viral kinetics and histopathological changes postchallenge in the lower and upper respiratory tracts of control (nonvaccinated but challenged) and protected NHPs. To our knowledge, this is the first published account of P.1 VOC challenge in NHPs.

RESULTS

Spike Antigen with Either Liquid or Lyophilized CoVaccine HT Elicits a Durable Humoral Response. A stably transformed *Drosophila* S2 cell line, without subculturing, yielded approximately 30 mg/L of the prefusion spike protein. Purification using CR3022 mAb immunoaffinity chromatography did not negatively affect the structural integrity of the purified protein (Figure S1A), and size-exclusion analysis revealed that the spike antigen is primarily homogeneous (Figure S1B).

To evaluate immunogenicity, 12 cynomolgus macaques were assigned into four groups (n = 3 per group) and received two immunizations with 5 (Group A) or 25 μg (Groups B and C) of the liquid prefusion spike trimer (S) antigen formulated with either the lyophilized (Groups A and C) or liquid (Group B) CoVaccine HT adjuvant or one dose of a colyophilized CoVaccine HT-adjuvanted control containing an unrelated viral glycoprotein antigen (Group D) (Figure 1A). The two doses were administered within a three-week interval, and all NHPs were challenged with the P.1 isolate 12 weeks postboost (~3 months, study week 15). Wuhan-Hu-1 S- and RBD-specific IgG titers were measured by a multiplexed microsphere immunoassay (MIA) using insect cell-expressed antigens coupled onto spectrally distinct, magnetic beads as described previously.[54] Serum S-specific IgG concentrations were interpolated using a standard curve generated from S-specific human IgG purified from vaccinated individuals (Figure 1B).

https://doi.org/10.1021/acsinfecdis.1c00600
ACS Infect. Dis. XXXX, XXX, XXX−XXX

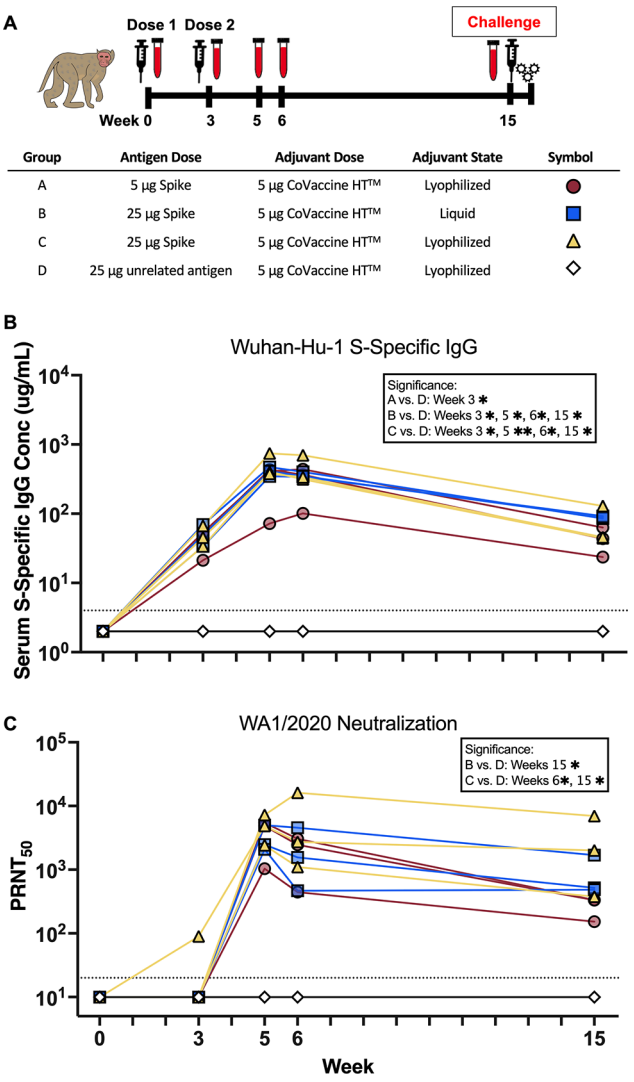

Group	Antigen Dose	Adjuvant Dose	Adjuvant State	Symbol
A	5 μg Spike	5 μg CoVaccine HT™	Lyophilized	●
B	25 μg Spike	5 μg CoVaccine HT™	Liquid	■
C	25 μg Spike	5 μg CoVaccine HT™	Lyophilized	▲
D	25 μg unrelated antigen	5 μg CoVaccine HT™	Lyophilized	◇

Figure 1. Vaccine scheme, IgG, and neutralizing antibody kinetics. (A) Twelve cynomolgus macaques were separated into four groups and given either 5 or 25 μg of the S protein formulated with either the liquid or reconstituted, lyophilized CoVaccine HT adjuvant. Two doses were administered IM three weeks apart, and the serum was collected at indicated time points. Macaques were challenged IN and IT with a total of 1×10^6 $TCID_{50}$ of the SARS-CoV-2 P.1 strain. (B) Serum Wuhan-Hu-1 S-specific IgG kinetics measured using a MIA with purified, human S-specific IgG standards to estimate serum concentration. Each sample was diluted 1:5000 and plotted as the average of duplicate measurements. Duplicate values varied by <10% of each other. The dotted line indicates the limit of quantification (LOQ, ≤4 μg/mL). Individual values falling below the LOQ were set to 1/2 LOQ. Significance was calculated using one-way ANOVA followed by Dunnett's multiple comparison to Group D at each time point. (C) WA1/2020 neutralizing antibody kinetics measured using a WT SARS-CoV-2 PRNT assay. Curve-fitted $PRNT_{50}$ titers were calculated using a sigmoidal dose−response curve. The dotted line indicates the limit of detection (LOD, ≤1:20). Individual values falling below the LOD were set to 1/2 LOD. Significance was calculated using the Kruskal−Wallis test followed by Dunn's multiple comparison ($^*p \leq 0.05$, $^{**}p \leq 0.01$).

RBD-specific IgG titers were read out as median fluorescence intensity (MFI) (Figure S2). All NHPs immunized with the adjuvanted S at both antigen doses seroconverted after the prime (week 3) with S-specific antibodies in the range of 20−70 μg/mL, and peak serum IgG concentrations were detected two weeks after the boost (week 5) in the range of 70−753 μg/mL. Macaques given a 25 μg dose of S demonstrated a greater IgG response to the antigen compared to those receiving 5 μg. RBD-specific IgG titers followed a similar trend. As expected, animals in Group D receiving an unrelated antigen did not develop any detectable S-specific IgG during this phase of the study. S-specific IgG remained detectable 12 weeks after the boost (week 15) although IgG concentrations dropped by 3.0- to 9.9-fold relative to the prior peak titer.

The titer of NtAb against the prototype WA1/2020 strain was determined using a standard PRNT with the wild-type (WT) virus (Figure 1C). NtAb from one animal in Group C was detectable after the prime (week 3). All S-immunized NHPs developed a potent neutralizing response, peaking two weeks after the boost (week 5) and generally remaining stable one week later (week 6). The group receiving 5 μg of the antigen showed the greatest variability. Nearly all immunized NHPs maintained neutralization capacity, with $PRNT_{50}$ greater than 1:150 dilution, 12 weeks after the final immunization (week 15). NtAbs from groups receiving 25 μg of S either remained stable or decreased up to 3.0-fold, while the group receiving 5 μg of S declined by ∼2.9−9.2-fold. A similar reduction in serum neutralization was also verified using a surrogate rVSV-SARS-CoV-2 S PRNT assay (Figure S3).

A Recombinant Subunit Vaccine Induces Stable Neutralizing Antibodies against VOCs. Circulating SARS-CoV-2 VOCs can evade vaccine-induced antibody responses and are associated with breakthrough infections in those fully immunized, especially as antibody titers wane.[55−61] To determine whether an adjuvanted, prototypic Wuhan-Hu-1 S subunit can generate durable cross-variant neutralizing antibodies, PRNTs using WT B.1.351, P.1, and B.1.617 isolates were determined with sera collected at the time of peak neutralization and 12 weeks after the final immunization, a time point at which antibody titers are expected to have waned. At week 6, potent neutralization of the B.1.351, P.1, and B.1.617 VOCs was detected, although 10.7-, 10.7-, and 5.7-fold lower, respectively, compared to WA1/2020 in all vaccine groups (Figure 2A). The decrease in neutralization against B.1.351 and B.1.617 is consistent with reports of titers in sera from NHPs and humans immunized with mRNA vaccines that show ∼8- and ∼5-fold reduction, respectively.[62−67] As antibody titers waned 10 weeks later (study week 15), the gap between neutralization titers against the WA1/2020 strain to the VOC isolates narrowed to 4.5-, 5.3-, and 5.1-fold differences, respectively (Figure 2B), driven by a proportionally larger decline in WA1/2020-specific neutralizing activity. At this later time point, all S-immunized macaques, except for a single macaque in Group A, maintained a detectable $PRNT_{50}$ titer greater than 1:40. A few macaques in Groups B and C demonstrated greater VOC neutralization at week 15 compared to week 6, suggesting a refinement or "maturation" of the humoral response toward neutralizing epitopes during this interval. Overall, 25 μg of the S protein generated a more durable and greater variant-neutralizing response than the lower antigen dose.

Immunization with Recombinant Subunits Reduces Viral Burden from Delayed P.1 (Gamma) Challenge. The characterization of the prototype strain and B.1.351 variant infections in NHP models has been described previously.[52,53,68−70] Here, we characterize the clinical signs and histological events of a P.1 VOC infection in cynomolgus

https://doi.org/10.1021/acsinfecdis.1c00600
ACS Infect. Dis. XXXX, XXX, XXX−XXX

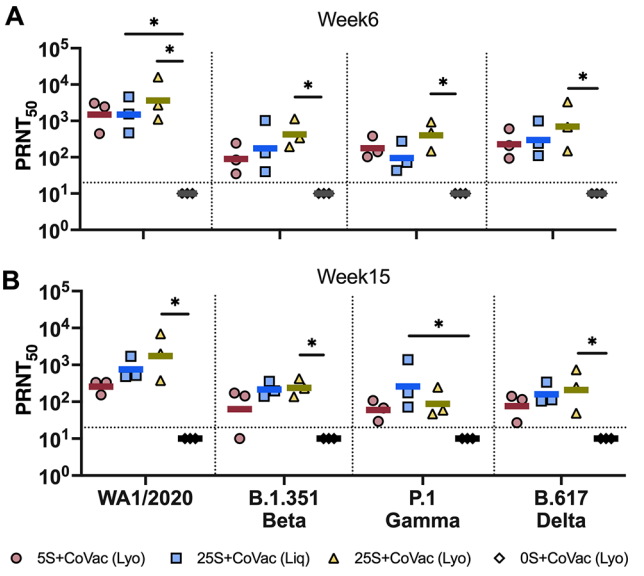

Figure 2. Cross-neutralizing antibody titers. Neutralizing antibody titers generated by 5 or 25 μg of the spike protein (S) formulated with either lyophilized (Lyo) or liquid (Liq) CoVaccine HT (CoVac) at (A) week 6 and (B) week 15 were measured using a WT SARS-CoV-2 PRNT assay with the WA1/2020, B.1.351 (Beta), P.1 (Gamma), and B.1.617 (Delta) VOCs. Curve-fitted $PRNT_{50}$ titers were calculated using a sigmoidal dose−response curve. Dotted lines indicate the LOD (≤1:20). Individual values falling below the LOD were set to 1/2 LOD. Significance was calculated using the Kruskal−Wallis test followed by Dunn's multiple comparison to Group D at each time point. Horizontal bars within the symbols mark the GMT of each group. Horizontal bars above the groups of symbols indicate the group comparisons, which showed statistically significant differences ($*p \leq 0.05$).

macaques and determine whether a prefusion spike subunit formulated with CoVaccine HT is effective at reducing the viral load against a circulating VOC after a 12-week interval following the final immunization. All NHPs were challenged with a total of 1×10^6 $TCID_{50}$ of the P.1 isolate using simultaneous intranasal and intratracheal inoculation routes. None of the NHPs challenged developed visible clinical signs of respiratory disease throughout the study, consistent with WA1/2020 strain-infected cynomolgus macaques.[52] No changes in the responsiveness, respiratory rate, respiratory effort, nasal or ocular discharge, or cough were documented during the observation period. The core body temperature also did not change. A slight, and sometimes intermittent, decrease in weight was observed in some macaques across all experimental groups; however, most returned to near the initial weight by day 14 (Figure S4A,B). A single control macaque in Group D had sustained weight loss throughout and at the end of the observation period. The weight change did not correlate with a higher viral load nor the degree of lung histopathology.

Bronchioalveolar lavages (BAL) from the lower respiratory tract and nasal and oral swabs (NS and OS, respectively) from the upper respiratory tract were collected at days 2, 4, 7, 10, and 14 after challenge to detect infectious virus, genomic RNA, or signs of viral replication. High levels of infectious virus, 5.8 and 5.0 $\log_{10}$ $TCID_{50}$ titers, were recovered two days postchallenge from the NS and BAL, respectively, from Group D control macaques (Figure 3A,D and Figure S5A,B).

Infectious virus continued to be detectable in both anatomic sites until at least day 7 postchallenge before becoming undetectable on day 10. All S-immunized NHPs presented $TCID_{50}$ titers at least 1−2 $\log_{10}$ lower than those of control macaques in both locations at all time points throughout the study, indicating a degree of protection conferred by both 5 and 25 μg S formulations of the subunit vaccine. Low levels of infectious virus in the BAL were recovered on day 2 in two out of the three macaques from both Groups A and B, while no culturable virus was recovered from all Group C macaques at any time point throughout the study. Except for a single macaque in Group B on day 4 only, no virus could be cultured from the BAL of any S-immunized macaques from this time point onward. Infectious virus from the NS was recoverable from immunized macaques throughout the study period and was variable between groups; however, these macaques on average had $TCID_{50}$ at least 1−2 $\log_{10}$ below those of control macaques. Only low levels of virus could be recovered on day 7 from two macaques from Group C before dropping to undetectable levels at day 10. No virus could be seen in Groups A and B from day 7 onward.

Quantitative RT-PCR was used as an additional measurement for the viral load. We detected the presence of viral RNA and viral replication throughout the 14-day study period in both the lower (Figure 3B,C and Figures S6A−C and S7A−C) and upper (Figure 3E,F and Figures S6D−F and S7D−F) respiratory airways and from the oral cavity (Figure 3G,H and Figures S6G−I and S7G−I). Quantification of viral RNA showed that both 5 and 25 μg immunization had reduced the viral load by approximately 1−2 $\log_{10}$ RNA copies/mL (or swab) over Group D control macaques, corroborating the $TCID_{50}$ results. Viral replication in most of the immunized macaques was low or undetectable by days 7 and 10 in the BAL and NS, respectively, which is 3−4 days earlier than in control macaques. Similarly, replication in the oral cavity was undetectable at least 3 days earlier in most of the S-immunized macaques than in the control group, suggesting a reduced potential for transmission. By contrast, high levels of viral RNA and replication, between 5 and 6 $\log_{10}$ RNA copies/mL, were observed in these control macaques before gradually resolving at day 10. Altogether, reduced viral loads and earlier clearance at all tested anatomic locations in Group A, B, and C macaques indicate a degree of durable protection from P.1 VOC infection provided by an adjuvanted protein subunit vaccine.

High-Dose Spike Antigen Reduces Lung Histopathology Caused by P.1 (Gamma) Challenge. To evaluate vaccine efficacy against COVID-19-like pathology, a section slide from each lung lobe and the bronchi was prepared from each macaque and stained with hematoxylin and eosin to survey for histopathological changes indicative of acute lung injury. The histopathological scoring system based on the presence/severity of edema, intra-alveolar and interstitial inflammation, perivascular lymphocytic cuffing, and an increased bronchiolar-associated lymphoid tissue (BALT) is outlined in Table S1. A cumulative average score was determined for each macaque based on the evaluation of these five characteristics per section for a total of 30 scores (Figure 4A). Significant differences in the cumulative average scores for each vaccine formulation vs controls were determined using one-way ANOVA followed by the Dunnett's multiple comparison test. Macaques in the control Group D appeared to have developed mild to moderate respiratory disease. The lower cumulative GMT scores of Groups B and C,

https://doi.org/10.1021/acsinfecdis.1c00600
ACS Infect. Dis. XXXX, XXX, XXX−XXX

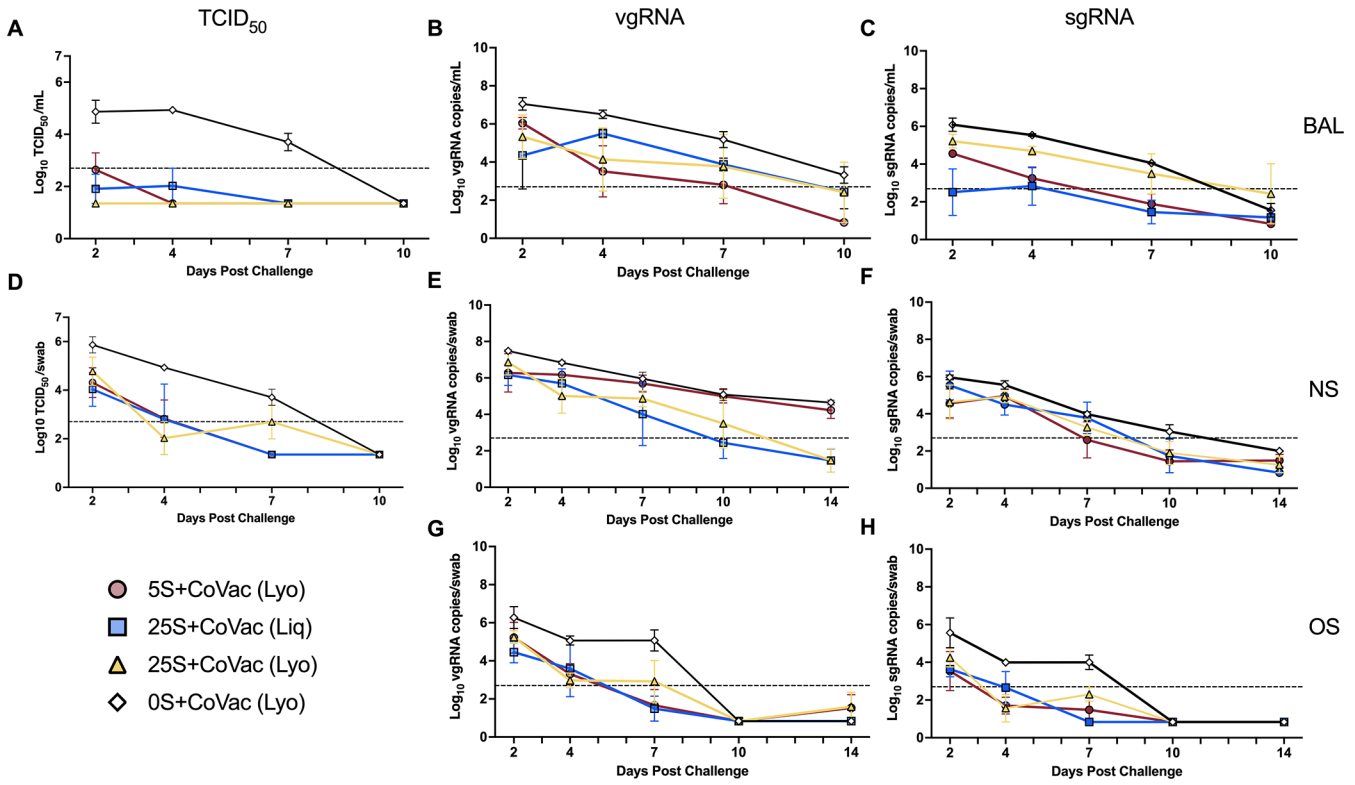

Figure 3. Viral load kinetics after P.1 challenge. Mean ± SEM of (A,D) $TCID_{50}$ titers, (B, E, and G) viral genomic, and (C, F, and H) subgenomic N RNA copies from (A−C) bronchoalveolar lavage (BAL), (D−F) nasal swab (NS), and (G,H) oral swab (OS) collected at the time points indicated. Dashed lines indicate the assay-specific LOD.

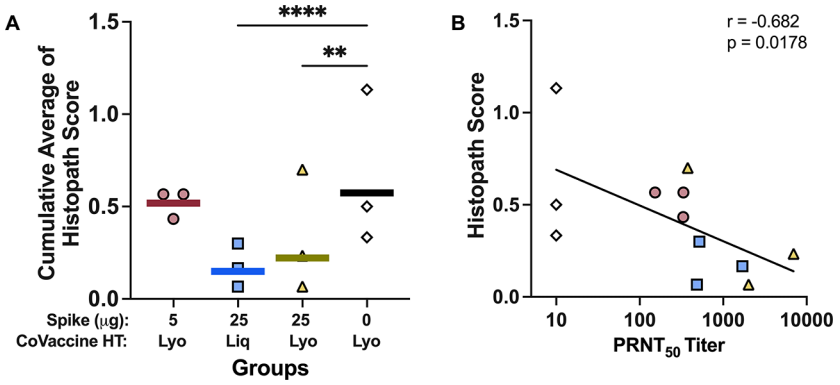

Figure 4. Histopathology score and correlation with neutralizing antibodies. (A) The cumulative average histopathology score was determined by averaging the scores of six sections cut from each lobe and the bronchi. The presence and severity of edema, intra-alveolar inflammation, perivascular cuffing, increased BALT, and interstitial inflammation were determined and assigned scores ranging from 0 to 3. Significant differences in lung histopathology were calculated using one-way ANOVA followed by Dunnett's multiple comparison to Group D with the scores from each section (30 scores per macaque) as replicates. Horizontal bars mark the GMT of each group (**$p \leq 0.01$, ****$p \leq 0.0001$). (B) Correlation between histopathology scores and WA1/2020-specific $PRNT_{50}$ titers were determined using the Spearman's correlation test.

immunized with 25 μg of S, suggest that these animals, except for a single macaque, were protected from lung pathology, while all Group A (immunized with 5 μg of S) macaques appeared to have developed mild disease despite exhibiting lower viral loads. Week 15 WA1/2020 NtAb levels were determined to be inversely correlated, although weakly, with histopathology scores using the Spearman's correlation test ($r = -0.682$, $p = 0.0178$) (Figure 4B). Week 15 prechallenge neutralizing antibody levels were lower in animals with higher histopathology scores, a trend seen with breakthrough infections in fully immunized individuals.[56] The moderate disease seen in the control animals is demonstrated in Figure 5A, where a representative low-power magnification shows a distribution of lymphocytic perivascular cuffing and clusters of intra-alveolar macrophages. In contrast, immunized animals (especially those receiving the higher antigen dose) appeared to have milder disease without these pathological changes (Figure 5B). For reference, a lung section from an uninfected macaque is shown in Figure S8. Macaques developing mild to moderate disease exhibited absent to moderate, focal and multifocal edema and perivascular cuffing with marked lymphocytic infiltration (Figure 6A−D). Syncytia of intra-alveolar multinucleated giant cells surrounded by acute and eosinophilic inflammatory infiltrates (Figure 6A) or increased

https://doi.org/10.1021/acsinfecdis.1c00600
ACS Infect. Dis. XXXX, XXX, XXX−XXX

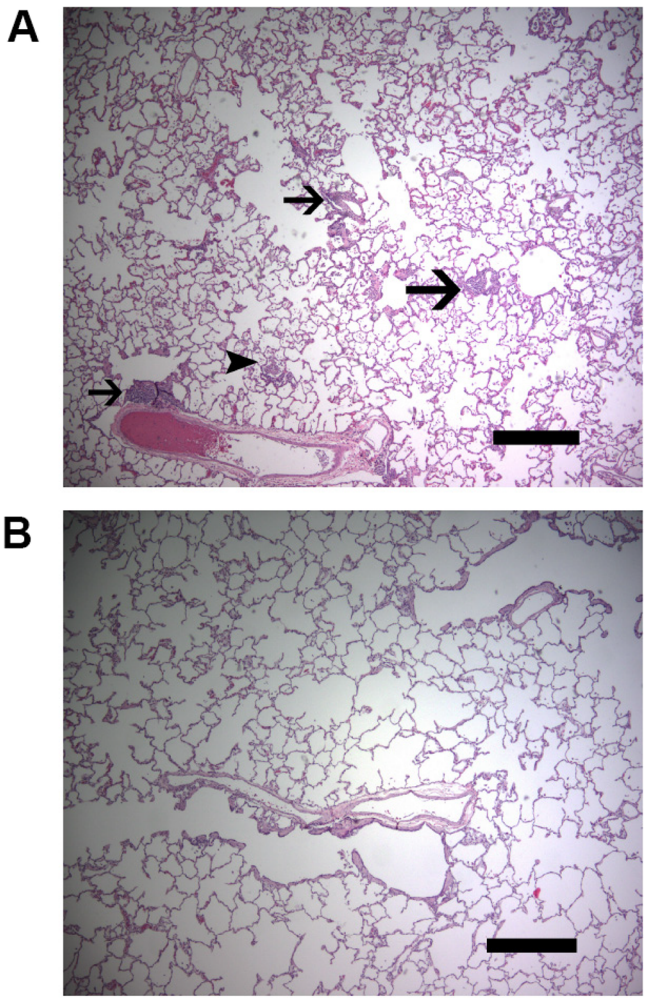

Figure 5. Histopathology observed in hematoxylin and eosin-stained lung sections of control cynomolgus macaques compared to immunized macaques after P.1 challenge. (A) Representative low-power view of a lung section showing distribution of lymphocytic perivascular cuffing (arrows) and clusters of intra-alveolar macrophages (arrowhead) in an unprotected macaque. (B) Representative low-power view of a lung section from an immunized macaque that did not exhibit pathologic changes. Scale bar = 500 μm.

intra-alveolar macrophages with interstitial lymphocytic inflammation, in addition to alveolar septal thickening and complete perivascular cuffing, can be seen in a moderately diseased control macaque (Figure 6B,C). A proteinaceous edema fluid filling alveolar spaces was also observed in unprotected macaques (Figure 6D). While these histopathological changes were also noticed in protected macaques, the findings appeared less severe (Figure 6E,F). A section from a protected macaque revealed a few intra-alveolar multinucleated giant cells without an increase in intra-alveolar macrophages, lymphocytic vascular cuffing, or interstitial inflammation (Figure 6E). Similarly, only partial lymphocytic perivascular cuffing with adjacent alveolar epithelial hyperplasia was noticed without an increased intraepithelial macrophage infiltrate and normal alveolar septal thickness in immunized macaques receiving 25 μg of S (Figure 6F).

P.1 Challenge Recalls a Broadly Neutralizing Anamnestic Response in Immunized Macaques and a Variant-Specific Primary Neutralizing Response in Naïve Macaques. To better understand the immunological basis of events happening after late challenge (12 weeks postbooster immunization) and to determine if P.1 challenge triggered an anamnestic response in immunized NHPs, postchallenge S-specific IgG concentrations and $PRNT_{50}$ titers were measured from sera collected upon necropsy at day 14 after challenge. Late P.1 challenge significantly boosted serum IgG concentrations to levels attained at the postimmunization peak at week 6, with less variance between animals, suggesting that a recall response was triggered by the heterologous infection (Figure 7A). Vaccine-matched (WA1/2020) and VOC-neutralizing (i.e., B.1.351, P.1, and B.1.617) antibody levels were also all significantly boosted to levels attaining or surpassing the peak levels generated through the initial immunization by 5-fold and higher than 20-fold, respectively (Figure 7B and Figure S3). Unsurprisingly, the greatest increase from prechallenge neutralization was against the P.1 challenge isolate. Group A showed slightly higher P.1 NtAbs than Group B and C macaques and was the only group to have significantly higher titers across different variants. The lower degree of histopathology seen in Groups B and C may indicate that 25 μg of S with either form of CoVaccine HT provides greater long-term protection. In Group D control macaques, P.1 challenge generated low levels of NtAbs compared to immunization alone, and it was only cross-reactive with the B.1.351 isolate and not to WA1/2020 nor B.1.617 isolates. This suggests that primary infection with one isolate of SARS-CoV-2 does not generate broad immunity against other variants in contrast to vaccine-derived immunity, which is more broadly cross-reactive with VOCs, even months after peak immunity is observed.

DISCUSSION

Understanding the durability and breadth of vaccine-generated immunity is critical for predicting long-term protection during the COVID-19 pandemic and for informing policy on strategic resource deployment to facilitate equitable vaccine access. Diversifying the types of vaccines currently used beyond mRNA and viral vectors to include other vaccine platforms, such as thermostable protein subunit vaccines,[71−73] can bolster global availability by mobilizing more vaccines to resource-poor areas, or overcoming antivector immunity and adverse effects, by using this platform as a booster to restore pre-existing natural or vaccine-induced immunity.[74−76]

We have demonstrated that two doses of a subunit vaccine consisting of a prefusion S trimer (Wuhan-Hu-1) formulated with liquid or lyophilized CoVaccine HT reduce the viral load and provide sufficient, durable, and cross-variant protection from mild to moderate disease lasting for at least three months after the final boost. This supports previous findings in rhesus macaques that S trimer-based subunit protein vaccines are highly immunogenic and generate long-lasting, robust antibody responses.[77] Furthermore, using a two-step purification method of immunoaffinity chromatography followed by a size-exclusion polishing step results in a homogeneous antigen composition and reduces host−cell carry-over plaguing conventional purification strategies for protein subunits.[78] Also promising is the prospect that the adjuvant, CoVaccine HT, can be lyophilized and reconstituted simply with water for injection and still retain its functionality. This technology has been previously used to develop mono- and multivalent filovirus vaccine formulations. Those studies demonstrated that single-vial, lyophilized formulations preserved the higher-order antigen structure and the biophysical properties of the

https://doi.org/10.1021/acsinfecdis.1c00600
ACS Infect. Dis. XXXX, XXX, XXX−XXX

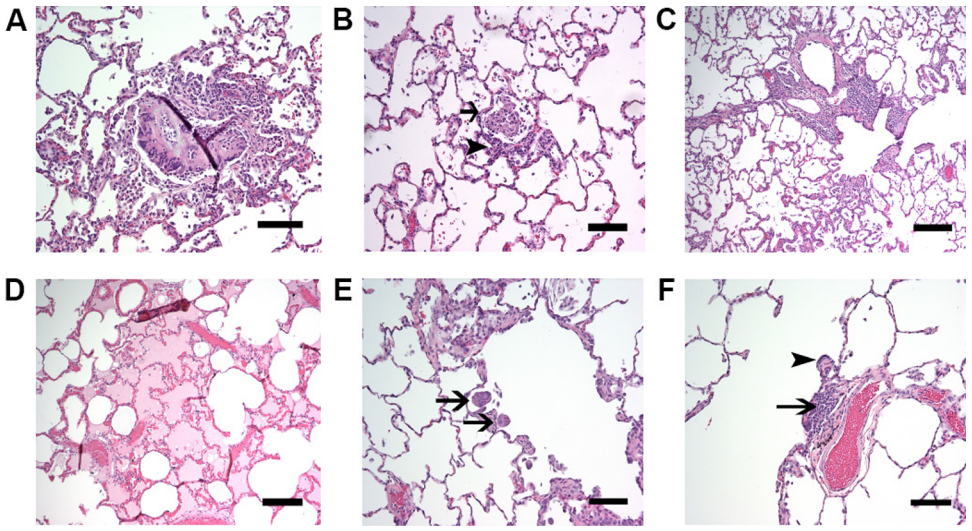

Figure 6. Histopathology observed in control cynomolgus macaques compared to that observed in immunized macaques after the P.1 challenge. (A–D) Unprotected macaques. (A) A syncytium of intra-alveolar multinucleated giant cells is seen surrounded by an acute and eosinophilic inflammatory infiltrate. (B) Increased intra-alveolar macrophages and an intra-alveolar multinucleated giant cell accompanied by interstitial lymphocytic inflammation and thickening. (C) Complete lymphocytic perivascular cuffing with increased intra-alveolar macrophages. (D) Proteinaceous edema fluid in alveolar spaces. (E,F) Protected macaques. (E) Intra-alveolar multinucleated giant cells (arrows) without increased intra-alveolar macrophages, lymphocytic vascular cuffing, or interstitial inflammation. (F) Partial lymphocytic perivascular cuff (arrow) with adjacent alveolar epithelial hyperplasia (arrowhead) without alveolar septal thickening. Scale bars = 10 (A–C, E, and F) and 20 μm (D).

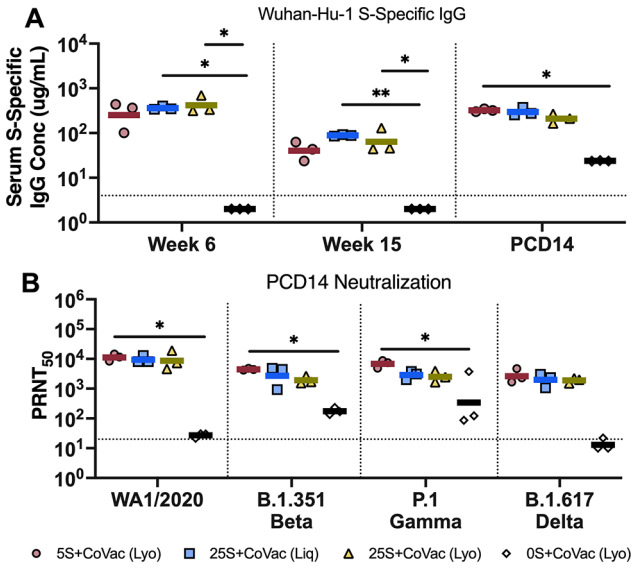

Figure 7. Postchallenge anamnestic response. (A) Vaccine-matched S-specific IgG concentrations from sera collected at week 6, week 15, and at 14 days postchallenge, measured by MIA. IgG concentrations were estimated using a human S-specific IgG standard as described previously. Horizontal bars mark the GMT for each group. The dotted line indicates the LOQ (≤4 μg/mL). Individual values falling below the LOQ were set to 1/2 LOQ. (B) Neutralizing antibodies 14 days after the P.1 challenge were measured using a WT SARS-CoV-2 PRNT assay with the WA1/2020, B.1.351 (Beta), P.1 (Gamma), and B.1.617 (Delta) VOCs. Curve-fitted $PRNT_{50}$ titers were calculated using a sigmoidal dose–response curve. The dotted line indicates the LOD (≤1:20). Individual values falling below the LOD were set to 1/2 LOD. Significance was calculated using the Kruskal–Wallis test followed by Dunn's multiple comparison to Group D at each time point ($*p \leq 0.05$, $**p \leq 0.01$).

adjuvant.[51] Robust levels of S-specific IgG and homologous as well as B.1.351, P.1, and B.1.617 cross-neutralizing antibodies were detected throughout the extended study period and inversely correlated with the viral load and lung damage. Neutralization against the B.1.351 and P.1 VOCs was equivalently reduced compared to the WA/2020 isolate immediately following the booster and suggested that E484K and N501Y may play a critical role in antibody evasion early on; however, this reduction equilibrated at the three-month time point across all VOCs tested while still affording sufficient protection. This report supports growing evidence that the Wuhan-Hu-1 S peptide sequence encoded by highly effective mRNA, viral-vectored, and subunit protein vaccines generates immunity that affords protection against circulating VOCs,[45,46,51,79,80] even months after the final vaccine dose when antibody titers are waning. Furthermore, we noticed that a few macaques receiving the higher antigen dose had developed increasingly potent cross-variant neutralizing titers immediately prior to viral challenge, which were greater than the titers observed during the peak humoral response. This suggests that a potentially remaining antigen depot or persistence of APCs may foster continued accumulation of somatic mutations and affinity maturation in memory B cells[81,82] beyond the initial vaccination phase.

This study is also the first to describe the course of infection and histopathology of a SARS-CoV-2 P.1 infection in an NHP model. Consistent with what was described in WA1/2020-infected cynomolgus macaques,[52,53] macaques challenged with the P.1 isolate did not develop an elevated temperature, nor did they show observable signs of respiratory disease. The viral load in the upper and lower respiratory tract peaked early during infection two days after challenge and gradually decreased to undetectable sgRNA levels by day 14 in unprotected animals, similar to viral kinetics described in another study using the same inoculating dose (1×10^6 $TCID_{50}$) but with an early pandemic isolate.[53] Although P.1 is estimated to be upwards of 2.4-fold more transmissible,[26] it is unclear whether the higher viral load observed during peak P.1 replication in this study compared to time-matched reports

https://doi.org/10.1021/acsinfecdis.1c00600
ACS Infect. Dis. XXXX, XXX, XXX–XXX

for a nonvariant isolate is a characteristic of P.1 replication or a discrepancy between readouts from different RT-PCR procedures. However, we show that immunization with both 5 and 25 μg doses of S effectively reduces the viral load in both upper and lower respiratory tracts, implying a lower likelihood of viral transmission even in mildly symptomatic macaques. Histopathological examination of lung and bronchial sections in unprotected macaques confirmed mild to moderate disease, which was abrogated in immunized macaques. COVID-19-like disease observed in this model consisted of increased intra-alveolar and interstitial infiltration, as well as giant syncytial cells, similar to previous observations.[52,64,83] While both high and low doses of the S antigen generate statistically negligible differences in humoral responses during peak immunity, it is clear from our findings that higher antigen doses, at least with CoVaccine HT, produce a more durable and protective response at later time points.

Late P.1 challenge induced an anamnestic response in all immunized macaques that restored S-specific antibody titers to peak serum concentrations seen shortly after the booster immunization and significantly enhanced vaccine-matched and VOC-neutralizing antibody titers. In most of the macaques receiving 25 μg of S, the immune recall occurred with little to no disease. The durability and cross-variant neutralizing nature of immune responses generated by mRNA and viral vectors have been documented up to six months or later.[63,84−86] However, breakthrough infections, particularly with variant strains, have been reported even in the presence of detectable and high-level NtAbs.[55,57,60,63,87] Anamnestic responses in fully immunized NHPs have been characterized previously with homologous and B.1.351 variant challenge and agree with our observations that viral challenge boosts functional antibody levels. Our analysis shows that viral challenge with a heterologous strain rapidly boosts not only homologous and challenge strain-specific NtAbs but also NtAbs against the unencountered variants, B.1.351 and B.1.617, underpinning the broad-spectrum potential of subunit protein vaccines. In contrast, control macaques, receiving no S antigen but infected with the P.1 variant, developed moderate levels of P.1 NtAbs that are only cross-neutralizing with B.1.351 and barely neutralize WA1/2020 and B.1.617, suggesting that natural infection with one variant of SARS-CoV-2 may confer only limited protection against other VOCs. Of course, further affinity maturation could not be observed here as the study ended 14 days after challenge.

The small size of our treatment groups ($n = 3$) is a limitation of our study and may therefore not provide enough statistical power to strongly correlate antibody concentrations to the viral load or the histopathology score. Furthermore, we cannot directly compare the outcome of our study to other studies that evaluate vaccine efficacy soon after the final immunization when immunity is greatest, as vaccine efficacy is known to decline over time. Likewise, we could not benchmark the efficacy of our vaccine formulation when the immunity is greatest at week 5; however, our late challenge scheme accurately reflects the current urgent need for decisions about timing and candidates for possible booster vaccinations during the pandemic situation as it provides useful information regarding the real-life durability and breadth of vaccine protection. Finally, while our results and evidence from other COVID-19 vaccine serological studies demonstrate that the prototypic spike sequence confers sufficient protection against B.1.351, P.1, and B.1.617 VOCs,[30,46,47,65,67,79] protection against highly divergent variants such as the BA.1 (Omicron) variant may require a second booster for greater coverage.[88−92] Further investigation is required to determine the full utility of protein vaccines to serve as a prime or boost in combination with other vaccines for this purpose.

In conclusion, we show that a two-dose regimen of a prefusion-stabilized trimeric S subunit protein vaccine formulated with the lyophilizable CoVaccine HT adjuvant reduces viral burden and high antigen doses can confer durable cross-variant immunity. Future efforts will therefore focus on developing a thermostabilized vaccine formulation in a single-vial format, potentially enabling facile worldwide distribution.

METHODS

Ethical Statement. The investigators adhered fully to the "Guide for the Care and Use of Laboratory Animals" by the Committee on Care of Laboratory Animal Resources Commission on Life Sciences, National Research Council. Cynomolgus macaques (*Macaca fascicularis*) were housed at BIOQUAL, Inc. (Rockville, MD). All macaque experiments were reviewed and approved by BIOQUAL's Animal Care and Use Committee. BIOQUAL, Inc. is accredited by the American Association for Accreditation of Laboratory Animal Care (AAALAC).

Study Design. Cynomolgus macaque studies were performed using three adjuvanted vaccine formulations and an adjuvanted control using an unrelated antigen: (A) 5 μg of the SARS-CoV-2 S protein with 5 mg of lyophilized CoVaccine HT, (B) 25 μg of the S protein with 5 mg of liquid CoVaccine HT, (C) 25 μg of the S protein with 5 mg of lyophilized CoVaccine HT, and (D) 25 μg of the Ebola virus (EBOV) glycoprotein with 5 mg of CoVaccine HT, colyophilized in one vial. CoVaccine HT (BTG International Ltd., London, United Kingdom) was lyophilized as previously described[51] and reconstituted with sterile water before mixing with the antigen. Each group consisted of both male and female cynomolgus macaques ($n = 3$ for each formulation) weighing between 2.8 and 8.2 kg. Cynomolgus macaques of Groups A−C were immunized intramuscularly (IM) in both deltoids (split dose) at weeks 0 and 3, and control animals were immunized only once at week 0. Prechallenge sera were collected at weeks 0, 3, 5, 6, and 15. Challenge at week 15 with the SARS-CoV-2 P.1 variant, hCoV-19/Japan/TY7-501/2021, and TY7-501 (BIOQUAL-generated stock [lot no. 031921-1215] in Calu-3 cells from seed stock no. TY7-501) was performed with an inoculum dose of 5×10^5 $TCID_{50}$/mL administered to each animal in volumes of 1 mL by intratracheal and intranasal injection at each site. Nasal and oral swabs (NS and OS, respectively) were collected on days 2, 4, 7, 10, and 14 after challenge. Bronchoalveolar lavage (BAL) samples were collected on days 2, 4, 7, and 10 after challenge. Necropsies and lung tissue collection were performed at the endpoint of the study at day 14 postchallenge. Samples were immediately processed and subsequently stored at −80 °C prior to analysis. S-specific serum IgG concentrations were determined using a microsphere immunoassay (MIA; see below). NtAbs were measured using wild-type and rVSV-SARS-CoV-2 S PRNTs (see below). The viral load in the NS, OS, and BAL was measured using plaque assays and quantification of genomic and subgenomic N transcript RNA (see below). Lung and bronchial tissues were processed and H&E-stained to delineate histopathological signs of disease in each animal.

https://doi.org/10.1021/acsinfecdis.1c00600
ACS Infect. Dis. XXXX, XXX, XXX−XXX

Recombinant Protein Expression and Purification. The plasmid was generated to express the prefusion, protease-resistant, and trimeric transmembrane (TM)-deleted spike (S) glycoprotein from SARS-CoV-2 as described previously.[54] Modifications to the gene include the removal of the furin and S2′ cleavage site, the addition of two prolines between the heptad repeat 1 and the central helix region, and a foldon trimerization domain. Briefly, *Drosophila* S2 cells were transfected with the S gene using Lipofectamine LTX with a PLUS reagent (Invitrogen, Carlsbad, CA) according to the manufacturer's instructions using ExCell420 media (Sigma-Aldrich, St. Louis, MO). Serial passage of the cell culture into fresh media spiked with 300 μg/mL hygromycin B generated a stably transformed cell line. To verify S protein expression, transformants were induced at a density of 1×10^6 cells/mL with culture medium containing 200 μM $CuSO_4$, and the supernatant was analyzed by sodium dodecyl sulfate polyacrylamide gel electrophoresis (SDS-PAGE) and Western blotting one week later. To scale up protein expression, the cell culture was expanded to 1 L in a 2 L Cellbag bioreactor on a WAVE bioreactor system (Cytiva, Marlborough, MA) and induced with 200 μM $CuSO_4$ the following day. The culture supernatant was harvested one week later, and sodium azide (Sigma-Aldrich, St. Louis, MO) was added up to 0.01% (w/v) before cold storage or purification.

The recombinant S protein was purified from clarified cell culture supernatants by immunoaffinity chromatography (IAC) using the SARS-CoV-2 cross-reactive mAb CR3022 (provided by Mapp Biopharmaceutical, RRID: AB_2848080) coupled to NHS-activated Sepharose at a concentration of 10 mg/mL. The antigen was eluted with a glycine buffer (pH 2) in tandem into a HiPrep 26/10 desalting column (Cytiva, Marlborough, MA) equilibrated with PBS. The oligomeric content was evaluated by size-exclusion chromatography using a HiLoad 16/600 column (GE Healthcare, Piscataway, NJ) equilibrated with PBS. The S protein was eluted as a single peak, and the final product migrated as two bands, corresponding to the monomer and the trimer on SDS-PAGE, under denaturing conditions, and was reactive to CR3022 mAb on a Western blot. Antigens were filter-sterilized with a 0.22 μm syringe filter (Cytiva, Marlborough, MA) and stored at −80 °C until use.

Analysis of Antibodies by Multiplex Microsphere Immunoassay. The IgG antibody titers in sera were measured using a multiplex microsphere-based immunoassay as described previously.[54,93−95] Spectrally distinct, magnetic MagPlex microspheres (Luminex Corporation, Austin, TX) were coupled to purified S, RBD, or bovine serum albumin (BSA). A mixture of the antigen-coupled beads was incubated with sera diluted with PBS + 1% BSA and 0.02% Tween 20 (PBS-BT) at 1:5,000 or 1:10,000 in black-sided 96-well plates for 3 h at 37 °C with agitation. Bound IgG was detected using 1 μg/mL red phycoerythrin (R-PE)-conjugated goat anti-human IgG antibodies (Jackson ImmunoResearch, Inc., West Grove, PA) and resuspended in a MAGPIX drive fluid before being analyzed on a MAGPIX Instrument (Luminex Corporation, Austin, TX).

To determine S-specific IgG concentrations in the sera, the median fluorescence intensity (MFI) readouts of each sample were interpolated against a standard curve generated using purified human IgG at concentrations in the range of 7.44−1000 ng/mL. To produce the antibody standard, IgG was purified from pooled sera of COVID-19-vaccinated human volunteers using protein A affinity chromatography followed by immunoaffinity chromatography (IAC) using NHS-Sepharose (Cytiva, Marlborough, MA) coupled with recombinant S to select for S-specific IgG. The purity was assessed using SDS-PAGE, and the antibody concentration was quantified using UV_{280} absorbance. The resulting MFI values were plotted against the $\log_{10}$-transformed concentrations and fitted using a sigmoidal dose−response, variable-slope model (GraphPad Prism, San Diego, CA). The resulting curves yielded r^2 values of >0.99 with a well-defined top and bottom and the linear range of the curve. The experimental S-specific IgG concentrations in experimental samples were determined by interpolation on the standard curves, multiplied by the dilution factor, and plotted as antibody concentrations (ng/mL).

Recombinant Vesicular Stomatitis Virus (rVSV) Neutralization Assay. Replication-competent rVSV expressing the SARS-CoV-2 S protein (Wuhan-Hu-1) was generated as described previously,[96] and the virus stocks were amplified in Vero E6 cells. For the plaque reduction neutralization test (PRNT), individual NHP serum samples were heat-inactivated at 56 °C for 30 min. Six 3-fold serial dilutions of serum samples, starting at 1:40 dilution, were prepared and incubated with 100 plaque-forming units (PFU) of rVSV-SARS-CoV-2 S at 37 °C for 1 h. Antibody−virus complexes were added to Vero cell monolayers in six-well plates and incubated at 37 °C for another hour followed by the addition of overlay media mixed with 1% agarose. Seventy-two hours later, cells were fixed and stained with a solution containing 1% formaldehyde, 1% methanol, and 0.05% crystal violet overnight for plaque enumeration. Neutralization titers ($PRNT_{50}$) were generated using a variable-slope, nonlinear regression, with upper and lower constraints (100 and 0% neutralization, respectively), using Prism 9 (GraphPad Software, San Diego, CA).

$TCID_{50}$ and Wild-Type SARS-CoV-2 Virus $PRNT_{50}$ Assay. $TCID_{50}$ and $PRNT_{50}$ assays were performed in a biosafety level 3 facility at BIOQUAL, Inc. (Rockville, MD). The $TCID_{50}$ assay was conducted by the addition of 10-fold graded dilutions of samples to Vero TMPRSS2 cell monolayers. Serial dilutions were performed in the cell culture wells in quadruplicates. Positive (virus stock of known infectious titer in the assay) and negative (medium only) control wells were included in each assay setup. The plates were incubated at 37 °C and 5.0% CO_2 for 4 days. The cell monolayers were visually inspected for CPE, i.e., complete destruction of the monolayer with cellular agglutination. The $TCID_{50}$ value was calculated using the Reed−Muench formula.[97] For samples that had less than three CPE positive wells on the first dilution, the $TCID_{50}$ could not be calculated using the Reed−Muench formula, and these samples were assigned a titer of below the limit of detection (i.e., <2.7 $\log_{10}$ $TCID_{50}$/mL). The $TCID_{50}$ value of the positive control should be within 2-fold of the expected value.

To measure neutralization, sera from each NHP were diluted to 1:10 followed by a 3-fold serial dilution. Diluted samples were then incubated with 30 plaque-forming units of wild-type SARS-CoV-2 USA-WA1/2020 (BEINR-52281), B.1.351 (BEI NR-55282), or P.1. (BEI NR-54982) variants, in an equal volume of culture medium for 1 h at 37 °C. The serum−virus mixtures were added to a monolayer of confluent Vero E6 cells and incubated for 1 h at 37 °C in 5% CO_2. Each well was then overlaid with culture medium containing 0.5% methylcellulose and incubated for three days at 37 °C in 5% CO_2. The plates were then fixed with methanol at −20 °C for

https://doi.org/10.1021/acsinfecdis.1c00600
ACS Infect. Dis. XXXX, XXX, XXX−XXX

30 min and stained with 0.2% crystal violet for 30 min at room temperature. $PRNT_{50}$ titers were calculated using a variable-slope, nonlinear regression, with upper and lower constraints (100 and 0% neutralization, respectively), on Prism 9 (GraphPad Software, San Diego, CA).

Histopathology. NHP lung tissue specimens from each lung lobe and bronchi were harvested at the time of necropsy and preserved in 10% formalin before processing and parafilm-embedded, fixed, and stained with hematoxylin and eosin. For each NHP, one section from the bronchi and one section from each lobe on the right and left lung were selected for scoring, for a total of six sections. Pathologic findings on each slide were scored on a scale of 0−2 for intra-alveolar edema, the amount of the BALT (bronchiolar-associated lymphoid tissue), and the presence of interstitial inflammation and 0−3 for perivascular inflammatory infiltrates (cuffing) and intra-alveolar inflammation (see Table S1.) Scores for the six slides from each macaque were tabulated, and a cumulative average score was calculated for each NHP using a total of 30 scores as replicates.

SARS-CoV-2 Viral Genomic and Subgenomic RNA Quantitative RT-PCR. The presence of viral RNA and viral replication in the BAL, NS, and OS after SARS-CoV-2 P.1 strain challenge was determined by quantitative RT-PCR. RNA was isolated from 200 μL of sample using a QIAamp MinElute Virus spin kit (Qiagen, Frederick, MD). To generate a control for the amplification reaction, RNA was isolated from the applicable virus stock using the same procedure. The number of copies for the control was calculated using known RNA weights per mol. A master mix was prepared containing Taq-polymerase, obtained from a TaqMan RT-PCR kit (Bioline catalog no. BIO-78005), RT, an RNAse inhibitor, a primer pair at a 2 μM concentration (2019-nCoV_N1-F: 5′-GAC CCC AAA ATC AGC GAA AT-3′ and 2019-nCoV_N1-R: 5′-TCT GGT TAC TGC CAG TTG AAT CTG-3′), and a probe (2019-nCoV_N1-P: 5′-FAM-ACC CCG CAT TAC GTT TGG TGG ACC-BHQ1-3′) at a concentration of 2 μM. For the reactions, 45 μL of the master mix and 5 μL of the sample RNA were added to the wells of a 96-well plate. All samples were tested in triplicate. Control RNA was prepared to contain 10^6−10^7 copies per 3 μL. Eight 10-fold serial dilutions of control RNA were prepared and produced a standard curve with a range of 1−10^7 copies per reaction. For amplification, the plate was placed in an Applied Biosystems 7500 sequence detector and amplified using the following program: 48 °C for 30 min, 95 °C for 10 min followed by 40 cycles of 95 °C for 15 s, and 1 min at 55 °C. Duplicate samples of each dilution were prepared as described above. If the copy number exceeded the upper detection limit, then the sample was diluted as needed. The number of copies of RNA per mL was calculated by interpolation from the standard curve and multiplying by the reciprocal of the 0.2 mL extraction volume. This gave a practical range of 50 to 5×10^8 RNA copies per mL for BAL samples, and for nasal and oral swabs, the viral loads were given per swab.

The RT-PCR assay for the sgRNA utilized primers and a probe specifically designed to amplify and bind to a region of the N gene mRNA from the coronavirus, which was not packaged into the virion. The signal was compared to a known standard curve of the plasmid containing the sequence of part of the messenger RNA and calculated to give copies per mL. The control RNA was prepared to contain 10^7 copies. Seven 10-fold serial dilutions of control RNA were prepared using Buffer AVE and generated a standard curve with a range of 1−10^6 copies/reaction. Duplicate samples of each dilution were prepared as described above with the primer pair (SG-N-F: CGATCTCTTGTAGATCTGTTCTC and SG-N-R: GGTGAACCAAGACG CAGTAT) and the probe (FAM-TAACCAGAATGGAGAACGCAGTGGG-BHQ). If the copy number exceeded the upper detection limit, then the sample was diluted as needed. For amplification, the plate was placed in an Applied Biosystems 7500 sequence detector and amplified using the following program: 48 °C for 30 min, 95 °C for 10 min followed by 40 cycles of 95 °C for 15 s, and 1 min at 55 °C. The number of copies of RNA per mL was calculated by interpolation from the standard curve and multiplying by the reciprocal of the 0.2 mL extraction volume. This gave a practical range of 50 to 5×10^7 RNA copies per mL for harvested samples.

Statistical Analysis. Statistically significant differences between the geometric mean of IgG concentrations or MFI in groups given different vaccine formulations at each time point were determined using two-way ANOVA followed by Dunnett's multiple comparison. Comparisons of $PRNT_{50}$ values between vaccine formulations were done using the Kruskal−Wallis test followed by the Dunn's multiple comparison test. Correlations between IgG or PRNT titers to the viral load in the BAL and NS were examined using the nonparametric Spearman's correlation test. Differences between histopathological scores in different treatment groups were calculated using one-way ANOVA followed by the Dunnett's multiple comparison test with the cumulative scores of all slides per macaque as replicates. All statistical analyses were completed using GraphPad Prism 9 software (San Diego, CA).

■ ASSOCIATED CONTENT

Supporting Information

The Supporting Information is available free of charge at https://pubs.acs.org/doi/10.1021/acsinfecdis.1c00600.

(Figure S1) Spike protein purification analysis; (Figure S2) serum Wuhan-Hu-1-specific IgG kinetics; (Figure S3) pre- and postchallenge rVSV-SARS-CoV-2 S neutralizing antibody response; (Figure S4) changes in weight postchallenge; (Figure S5) individual $TCID_{50}$ viral load from the BAL and NS serial diluted samples from the lower and upper respiratory tract at each time point; (Figure S6) individual genomic viral RNA load samples collected from the BAL, nasal, and oral swab from each macaque at each time point and the viral genomic RNA quantified using qPCR; (Figure S7) individual subgenomic N transcript viral RNA load samples collected from the BAL, nasal, and oral swab from each macaque at each time point and the subgenomic N transcript RNA quantified using qPCR; (Figure S8) section from the lungs of an uninfected cynomolgus macaque (PDF)

■ AUTHOR INFORMATION

Corresponding Author

Axel T. Lehrer − *Department of Tropical Medicine, Medical Microbiology, and Pharmacology, John A. Burns School of Medicine, University of Hawai'i at Mānoa, Honolulu, Hawaii 96813, United States*; Email: lehrer@hawaii.edu

https://doi.org/10.1021/acsinfecdis.1c00600
ACS Infect. Dis. XXXX, XXX, XXX−XXX

Authors

Albert To − *Department of Tropical Medicine, Medical Microbiology, and Pharmacology, John A. Burns School of Medicine, University of Hawai'i at Mānoa, Honolulu, Hawaii 96813, United States;* orcid.org/0000-0002-7118-9803

Teri Ann S. Wong − *Department of Tropical Medicine, Medical Microbiology, and Pharmacology, John A. Burns School of Medicine, University of Hawai'i at Mānoa, Honolulu, Hawaii 96813, United States*

Michael M. Lieberman − *Department of Tropical Medicine, Medical Microbiology, and Pharmacology, John A. Burns School of Medicine, University of Hawai'i at Mānoa, Honolulu, Hawaii 96813, United States*

Karen Thompson − *Department of Pathology, John A. Burns School of Medicine, University of Hawai'i at Mānoa, Honolulu, Hawaii 96813, United States*

Aquena H. Ball − *Department of Tropical Medicine, Medical Microbiology, and Pharmacology, John A. Burns School of Medicine, University of Hawai'i at Mānoa, Honolulu, Hawaii 96813, United States*

Laurent Pessaint − *BIOQUAL, Inc., Rockville, Maryland 20850, United States*

Jack Greenhouse − *BIOQUAL, Inc., Rockville, Maryland 20850, United States*

Nisrine Daham − *BIOQUAL, Inc., Rockville, Maryland 20850, United States*

Anthony Cook − *BIOQUAL, Inc., Rockville, Maryland 20850, United States*

Brandon Narvaez − *BIOQUAL, Inc., Rockville, Maryland 20850, United States*

Zack Flinchbaugh − *BIOQUAL, Inc., Rockville, Maryland 20850, United States*

Alex Van Ry − *BIOQUAL, Inc., Rockville, Maryland 20850, United States*

Jake Yalley-Ogunro − *BIOQUAL, Inc., Rockville, Maryland 20850, United States*

Hanne Andersen Elyard − *BIOQUAL, Inc., Rockville, Maryland 20850, United States*

Chih-Yun Lai − *Department of Tropical Medicine, Medical Microbiology, and Pharmacology, John A. Burns School of Medicine, University of Hawai'i at Mānoa, Honolulu, Hawaii 96813, United States*

Oreola Donini − *Soligenix, Inc., Princeton, New Jersey 08540, United States*

Complete contact information is available at: https://pubs.acs.org/10.1021/acsinfecdis.1c00600

Author Contributions

A.T., M.M.L., H.A.E., O.D., and A.T.L. conceptualized the study; A.T., T.A.S.W., K.T., A.H.B., L.P., H.A.E., C.-Y.L., and A.T.L. developed the methodology; A.T., T.A.S.W., K.T.,L.P., J.G., N.D., A.C., B.N., Z.F., A.V.R., and J.Y.-O. performed the experiments; A.T., M.M.L., K.T., and A.T.L. performed the formal analysis; A.T., K.T., and A.H.B. performed the visualization; O.D. and A.T.L. acquired the project funding; H.A.E., O.D., and A.T.L. administrated the project; H.A.E., O.D., and A.T.L. supervised the study; A.T., M.M.L., K.T., and A.T.L. wrote the original draft; A.T., T.A.S.W., M.M.L., K.T., A.H.B., H.A.E., O.D., and A.T.L. reviewed and edited the manuscript.

Funding

This work was supported by the National Institute of Allergy and Infectious Diseases Grant R01AI132323 (A.T.L.), the National Heart, Lung, and Blood Institute Grant T32HL115505-09, the National Institute of Minority Health and Health Disparities Grant U54MD007601, the National Institute of General Medical Sciences Grant P30GM114737, and institutional funds from the University of Hawai'i at Mānoa, BIOQUAL, Inc., and Soligenix, Inc.

Notes

The authors declare the following competing financial interest(s): ATL and OD are named inventors on a patent application covering a recombinant subunit vaccine for SARS-CoV-2. LP, JG, ND, AC, BN, ZF, AVR, JYO and HAE are current employees of BIOQUAL, Inc. OD is a current employee of Soligenix Inc. All other authors declare no competing interests.

All data are available in the main text or the supplementary materials.

■ ACKNOWLEDGMENTS

We would like to thank Kendall B. Preston from the University of Colorado Boulder, USA, for lyophilizing our CoVaccine HT adjuvant, Takaji Wakita from the National Institute of Infectious Diseases, Japan, for the P.1 viral challenge strain, and Shelby O'Connor and John Baczenas from the University of Wisconsin-Madison, USA, for deep sequencing our in-house viral stock. We also would like to thank Adrian Creanga from the Vaccine Research Center-NIAID, USA, for the Vero TMPRSS2 cell line used in our $TCID_{50}$ and $PRNT_{50}$ assays as well as Andrea Marzi, Laboratory of Virology, NIAID-NIH, USA, for the rVSV-SARS-CoV 2 virus stock used in our surrogate $PRNT_{50}$ assay. Furthermore, we would like to thank Melissa Hamilton, the study coordinator at BIOQUAL, Inc., USA; Mapp Biopharmaceutical, Inc. for the CR3022 mAb used for protein purification; BTG International Limited for the CoVaccine HT adjuvant; and Miyoko Bellinger and Kristen Ewall from the JABSOM Histocore for preparing lung tissue sections for histopathological analysis. The graphical abstract was generated using Biorender.com.

■ REFERENCES

(1) Zhou, P.; Yang, X. L.; Wang, X. G.; Hu, B.; Zhang, L.; Zhang, W.; Si, H. R.; Zhu, Y.; Li, B.; Huang, C. L.; Chen, H. D.; Chen, J.; Luo, Y.; Guo, H.; Jiang, R. D.; Liu, M. Q.; Chen, Y.; Shen, X. R.; Wang, X.; Zheng, X. S.; Zhao, K.; Chen, Q. J.; Deng, F.; Liu, L. L.; Yan, B.; Zhan, F. X.; Wang, Y. Y.; Xiao, G. F.; Shi, Z. L. A pneumonia outbreak associated with a new coronavirus of probable bat origin. *Nature* **2020**, *579*, 270−273.

(2) Zhu, N.; Zhang, D.; Wang, W.; Li, X.; Yang, B.; Song, J.; Zhao, X.; Huang, B.; Shi, W.; Lu, R.; Niu, P.; Zhan, F.; Ma, X.; Wang, D.; Xu, W.; Wu, G.; Gao, G. F.; Tan, W.; China Novel Coronavirus Investigating and Research Team. A Novel Coronavirus from Patients with Pneumonia in China, 2019. *N. Engl. J. Med.* **2020**, *382*, 727−733.

(3) Garg, S.; Singh, M. M.; Deshmukh, C. P.; Bhatnagar, N.; Borle, A. L.; Kumar, R. Critical interpretative synthesis of herd immunity for COVID-19 pandemic. *J. Family Med. Prim. Care* **2021**, *10*, 1117−1123.

(4) Huang, C.; Wang, Y.; Li, X.; Ren, L.; Zhao, J.; Hu, Y.; Zhang, L.; Fan, G.; Xu, J.; Gu, X.; Cheng, Z.; Yu, T.; Xia, J.; Wei, Y.; Wu, W.; Xie, X.; Yin, W.; Li, H.; Liu, M.; Xiao, Y.; Gao, H.; Guo, L.; Xie, J.; Wang, G.; Jiang, R.; Gao, Z.; Jin, Q.; Wang, J.; Cao, B. Clinical features of patients infected with 2019 novel coronavirus in Wuhan, China. *Lancet* **2020**, *395*, 497−506.

(5) Wu, Z.; McGoogan, J. M. Characteristics of and Important Lessons From the Coronavirus Disease 2019 (COVID-19) Outbreak in China: Summary of a Report of 72314 Cases From the Chinese Center for Disease Control and Prevention. *JAMA* **2020**, *323*, 1239−1242.
(6) Helms, J.; Kremer, S.; Merdji, H.; Clere-Jehl, R.; Schenck, M.; Kummerlen, C.; Collange, O.; Boulay, C.; Fafi-Kremer, S.; Ohana, M.; Anheim, M.; Meziani, F. Neurologic Features in Severe SARS-CoV-2 Infection. *N. Engl. J. Med.* **2020**, *382*, 2268−2270.
(7) Levi, M.; Thachil, J.; Iba, T.; Levy, J. H. Coagulation abnormalities and thrombosis in patients with COVID-19. *Lancet Haematol.* **2020**, *7*, e438−e440.
(8) Mao, R.; Qiu, Y.; He, J. S.; Tan, J. Y.; Li, X. H.; Liang, J.; Shen, J.; Zhu, L. R.; Chen, Y.; Iacucci, M.; Ng, S. C.; Ghosh, S.; Chen, M. H. Manifestations and prognosis of gastrointestinal and liver involvement in patients with COVID-19: a systematic review and meta-analysis. *Lancet Gastroenterol. Hepatol.* **2020**, *5*, 667−678.
(9) Richardson, S.; Hirsch, J. S.; Narasimhan, M.; Crawford, J. M.; McGinn, T.; Davidson, K. W.; Northwell COVID-19 Research Consortium. Presenting Characteristics, Comorbidities, and Outcomes Among 5700 Patients Hospitalized With COVID-19 in the New York City Area. *JAMA* **2020**, *323*, 2052−2059.
(10) Bai, Y.; Yao, L.; Wei, T.; Tian, F.; Jin, D. Y.; Chen, L.; Wang, M. Presumed Asymptomatic Carrier Transmission of COVID-19. *JAMA* **2020**, *323*, 1406−1407.
(11) Ganyani, T.; Kremer, C.; Chen, D.; Torneri, A.; Faes, C.; Wallinga, J.; Hens, N. Estimating the generation interval for coronavirus disease (COVID-19) based on symptom onset data, March 2020. *Euro. Surveill.* **2020**, *25*, 2000257.
(12) He, X.; Lau, E. H. Y.; Wu, P.; Deng, X.; Wang, J.; Hao, X.; Lau, Y. C.; Wong, J. Y.; Guan, Y.; Tan, X.; Mo, X.; Chen, Y.; Liao, B.; Chen, W.; Hu, F.; Zhang, Q.; Zhong, M.; Wu, Y.; Zhao, L.; Zhang, F.; Cowling, B. J.; Li, F.; Leung, G. M. Temporal dynamics in viral shedding and transmissibility of COVID-19. *Nat. Med.* **2020**, *26*, 672−675.
(13) He, Z.; Ren, L.; Yang, J.; Guo, L.; Feng, L.; Ma, C.; Wang, X.; Leng, Z.; Tong, X.; Zhou, W.; Wang, G.; Zhang, T.; Guo, Y.; Wu, C.; Wang, Q.; Liu, M.; Wang, C.; Jia, M.; Hu, X.; Wang, Y.; Zhang, X.; Hu, R.; Zhong, J.; Yang, J.; Dai, J.; Chen, L.; Zhou, X.; Wang, J.; Yang, W.; Wang, C. Seroprevalence and humoral immune durability of anti-SARS-CoV-2 antibodies in Wuhan, China: a longitudinal, population-level, cross-sectional study. *Lancet* **2021**, *397*, 1075−1084.
(14) Ibarrondo, F. J.; Fulcher, J. A.; Goodman-Meza, D.; Elliott, J.; Hofmann, C.; Hausner, M. A.; Ferbas, K. G.; Tobin, N. H.; Aldrovandi, G. M.; Yang, O. O. Rapid Decay of Anti-SARS-CoV-2 Antibodies in Persons with Mild Covid-19. *N. Engl. J. Med.* **2020**, *383*, 1085−1087.
(15) Rodda, L. B.; Netland, J.; Shehata, L.; Pruner, K. B.; Morawski, P. A.; Thouvenel, C. D.; Takehara, K. K.; Eggenberger, J.; Hemann, E. A.; Waterman, H. R.; Fahning, M. L.; Chen, Y.; Hale, M.; Rathe, J.; Stokes, C.; Wrenn, S.; Fiala, B.; Carter, L.; Hamerman, J. A.; King, N. P.; Gale, M., Jr.; Campbell, D. J.; Rawlings, D. J.; Pepper, M. Functional SARS-CoV-2-Specific Immune Memory Persists after Mild COVID-19. *Cell* **2021**, *184*, 169−183 e117.
(16) Khoury, D. S.; Cromer, D.; Reynaldi, A.; Schlub, T. E.; Wheatley, A. K.; Juno, J. A.; Subbarao, K.; Kent, S. J.; Triccas, J. A.; Davenport, M. P. Neutralizing antibody levels are highly predictive of immune protection from symptomatic SARS-CoV-2 infection. *Nat. Med.* **2021**, *27*, 1205−1211.
(17) Seow, J.; Graham, C.; Merrick, B.; Acors, S.; Pickering, S.; Steel, K. J. A.; Hemmings, O.; O'Byrne, A.; Kouphou, N.; Galao, R. P.; Betancor, G.; Wilson, H. D.; Signell, A. W.; Winstone, H.; Kerridge, C.; Huettner, I.; Jimenez-Guardeno, J. M.; Lista, M. J.; Temperton, N.; Snell, L. B.; Bisnauthsing, K.; Moore, A.; Green, A.; Martinez, L.; Stokes, B.; Honey, J.; Izquierdo-Barras, A.; Arbane, G.; Patel, A.; Tan, M. K. I.; O'Connell, L.; O'Hara, G.; MacMahon, E.; Douthwaite, S.; Nebbia, G.; Batra, R.; Martinez-Nunez, R.; Shankar-Hari, M.; Edgeworth, J. D.; Neil, S. J. D.; Malim, M. H.; Doores, K. J. Longitudinal observation and decline of neutralizing antibody responses in the three months following SARS-CoV-2 infection in humans. *Nat. Microbiol.* **2020**, *5*, 1598−1607.
(18) Wheatley, A. K.; Juno, J. A.; Wang, J. J.; Selva, K. J.; Reynaldi, A.; Tan, H. X.; Lee, W. S.; Wragg, K. M.; Kelly, H. G.; Esterbauer, R.; Davis, S. K.; Kent, H. E.; Mordant, F. L.; Schlub, T. E.; Gordon, D. L.; Khoury, D. S.; Subbarao, K.; Cromer, D.; Gordon, T. P.; Chung, A. W.; Davenport, M. P.; Kent, S. J. Evolution of immune responses to SARS-CoV-2 in mild-moderate COVID-19. *Nat. Commun.* **2021**, *12*, 1162.
(19) Gupta, V.; Bhoyar, R. C.; Jain, A.; Srivastava, S.; Upadhayay, R.; Imran, M.; Jolly, B.; Divakar, M. K.; Sharma, D.; Sehgal, P.; Ranjan, G.; Gupta, R.; Scaria, V.; Sivasubbu, S. Asymptomatic reinfection in two healthcare workers from India with genetically distinct SARS-CoV-2. *Clin. Infect. Dis.* **2021**, *73*, e2823−e2825.
(20) Harrington, D.; Kele, B.; Pereira, S.; Couto-Parada, X.; Riddell, A.; Forbes, S.; Dobbie, H.; Cutino-Moguel, T. Confirmed Reinfection with SARS-CoV-2 Variant VOC-202012/01. *Clin. Infect. Dis.* **2021**, *73*, 1946−1947.
(21) Loconsole, D.; Sallustio, A.; Accogli, M.; Centrone, F.; Casulli, D.; Madaro, A.; Tedeschi, E.; Parisi, A.; Chironna, M. Symptomatic SARS-CoV-2 Reinfection in a Healthy Healthcare Worker in Italy Confirmed by Whole-Genome Sequencing. *Viruses* **2021**, *13*, 899.
(22) Prado-Vivar, B.; Becerra-Wong, M.; Guadalupe, J. J.; Márquez, S.; Gutierrez, B.; Rojas-Silva, P.; Grunauer, M.; Trueba, G.; Barragan, V.; Cardenas, P. A case of SARS-CoV-2 reinfection in Ecuador. *Lancet Infect. Dis.* **2021**, *21*, No. e142.
(23) Tillett, R. L.; Sevinsky, J. R.; Hartley, P. D.; Kerwin, H.; Crawford, N.; Gorzalski, A.; Laverdure, C.; Verma, S. C.; Rossetto, C. C.; Jackson, D.; Farrell, M. J.; Van Hooser, S.; Pandori, M. Genomic evidence for reinfection with SARS-CoV-2: a case study. *Lancet Infect. Dis.* **2021**, *21*, 52−58.
(24) Johnson, B. A.; Xie, X.; Bailey, A. L.; Kalveram, B.; Lokugamage, K. G.; Muruato, A.; Zou, J.; Zhang, X.; Juelich, T.; Smith, J. K.; Zhang, L.; Bopp, N.; Schindewolf, C.; Vu, M.; Vanderheiden, A.; Winkler, E. S.; Swetnam, D.; Plante, J. A.; Aguilar, P.; Plante, K. S.; Popov, V.; Lee, B.; Weaver, S. C.; Suthar, M. S.; Routh, A. L.; Ren, P.; Ku, Z.; An, Z.; Debbink, K.; Diamond, M. S.; Shi, P. Y.; Freiberg, A. N.; Menachery, V. D. Loss of furin cleavage site attenuates SARS-CoV-2 pathogenesis. *Nature* **2021**, *591*, 293−299.
(25) Plante, J. A.; Liu, Y.; Liu, J.; Xia, H.; Johnson, B. A.; Lokugamage, K. G.; Zhang, X.; Muruato, A. E.; Zou, J.; Fontes-Garfias, C. R.; Mirchandani, D.; Scharton, D.; Bilello, J. P.; Ku, Z.; An, Z.; Kalveram, B.; Freiberg, A. N.; Menachery, V. D.; Xie, X.; Plante, K. S.; Weaver, S. C.; Shi, P. Y. Spike mutation D614G alters SARS-CoV-2 fitness. *Nature* **2021**, *592*, 116−121.
(26) Faria, N. R.; Mellan, T. A.; Whittaker, C.; Claro, I. M.; Candido, D. D. S.; Mishra, S.; Crispim, M. A. E.; Sales, F. C. S.; Hawryluk, I.; McCrone, J. T.; Hulswit, R. J. G.; Franco, L. A. M.; Ramundo, M. S.; de Jesus, J. G.; Andrade, P. S.; Coletti, T. M.; Ferreira, G. M.; Silva, C. A. M.; Manuli, E. R.; Pereira, R. H. M.; Peixoto, P. S.; Kraemer, M. U. G.; Gaburo, N., Jr.; Camilo, C. D. C.; Hoeltgebaum, H.; Souza, W. M.; Rocha, E. C.; de Souza, L. M.; de Pinho, M. C.; Araujo, L. J. T.; Malta, F. S. V.; de Lima, A. B.; Silva, J. D. P.; Zauli, D. A. G.; Ferreira, A. C. S.; Schnekenberg, R. P.; Laydon, D. J.; Walker, P. G. T.; Schluter, H. M.; Dos Santos, A. L. P.; Vidal, M. S.; Del Caro, V. S.; Filho, R. M. F.; Dos Santos, H. M.; Aguiar, R. S.; Proenca-Modena, J. L.; Nelson, B.; Hay, J. A.; Monod, M.; Miscouridou, X.; Coupland, H.; Sonabend, R.; Vollmer, M.; Gandy, A.; Prete, C. A., Jr.; Nascimento, V. H.; Suchard, M. A.; Bowden, T. A.; Pond, S. L. K.; Wu, C. H.; Ratmann, O.; Ferguson, N. M.; Dye, C.; Loman, N. J.; Lemey, P.; Rambaut, A.; Fraiji, N. A.; Carvalho, M.; Pybus, O. G.; Flaxman, S.; Bhatt, S.; Sabino, E. C. Genomics and epidemiology of the P.1 SARS-CoV-2 lineage in Manaus, Brazil. *Science* **2021**, *372*, 815−821.
(27) Mlcochova, P.; Kemp, S.; Dhar, M. S.; Papa, G.; Meng, B.; Ferreira, I.; Datir, R.; Collier, D. A.; Albecka, A.; Singh, S.; Pandey, R.; Brown, J.; Zhou, J.; Goonawardane, N.; Mishra, S.; Whittaker, C.; Mellan, T.; Marwal, R.; Datta, M.; Sengupta, S.; Ponnusamy, K.; Radhakrishnan, V. S.; Abdullahi, A.; Charles, O.; Chattopadhyay, P.;

https://doi.org/10.1021/acsinfecdis.1c00600
ACS Infect. Dis. XXXX, XXX, XXX−XXX

Devi, P.; Caputo, D.; Peacock, T.; Wattal, D. C.; Goel, N.; Satwik, A.; Vaishya, R.; Agarwal, M.; The Indian SARS-CoV-2 Genomics Consortium; The Genotype to Phenotype Japan (G2P-Japan) Consortium; The CITIID-NIHR BioResource COVID-19 Collaboration; Mavousian, A.; Lee, J. H.; Bassi, J.; Silacci-Fegni, C.; Saliba, C.; Pinto, D.; Irie, T.; Yoshida, I.; Hamilton, W. L.; Sato, K.; Bhatt, S.; Flaxman, S.; James, L. C.; Corti, D.; Piccoli, L.; Barclay, W. S.; Rakshit, P.; Agrawal, A.; Gupta, R. K. SARS-CoV-2 B.1.617.2 Delta variant replication and immune evasion. *Nature* **2021**, *599*, 114−119.

(28) Sabino, E. C.; Buss, L. F.; Carvalho, M. P. S.; Prete, C. A., Jr.; Crispim, M. A. E.; Fraiji, N. A.; Pereira, R. H. M.; Parag, K. V.; da Silva Peixoto, P.; Kraemer, M. U. G.; Oikawa, M. K.; Salomon, T.; Cucunuba, Z. M.; Castro, M. C.; de Souza Santos, A. A.; Nascimento, V. H.; Pereira, H. S.; Ferguson, N. M.; Pybus, O. G.; Kucharski, A.; Busch, M. P.; Dye, C.; Faria, N. R. Resurgence of COVID-19 in Manaus, Brazil, despite high seroprevalence. *Lancet* **2021**, *397*, 452−455.

(29) FDA. *Fact Sheet for Health Care Providers Emergency Use Authorization (EDA) of Bamlanivimab and Etesevimab*. 2021. https://www.fda.gov/media/145802/download (accessed.

(30) Wang, Z.; Schmidt, F.; Weisblum, Y.; Muecksch, F.; Barnes, C. O.; Finkin, S.; Schaefer-Babajew, D.; Cipolla, M.; Gaebler, C.; Lieberman, J. A.; Oliveira, T. Y.; Yang, Z.; Abernathy, M. E.; Huey-Tubman, K. E.; Hurley, A.; Turroja, M.; West, K. A.; Gordon, K.; Millard, K. G.; Ramos, V.; Da Silva, J.; Xu, J.; Colbert, R. A.; Patel, R.; Dizon, J.; Unson-O'Brien, C.; Shimeliovich, I.; Gazumyan, A.; Caskey, M.; Bjorkman, P. J.; Casellas, R.; Hatziioannou, T.; Bieniasz, P. D.; Nussenzweig, M. C. mRNA vaccine-elicited antibodies to SARS-CoV-2 and circulating variants. *Nature* **2021**, *592*, 616−622.

(31) Brehm, T. T.; Pfefferle, S.; von Possel, R.; Kobbe, R.; Nörz, D.; Schmiedel, S.; Grundhoff, A.; Olearo, F.; Emmerich, P.; Robitaille, A.; Gunther, T.; Braun, P.; Andersen, G.; Knobloch, J. K.; Addo, M. M.; Lohse, A. W.; Aepfelbacher, M.; Fischer, N.; Schulze Zur Wiesch, J.; Lutgehetmann, M. SARS-CoV-2 Reinfection in a Healthcare Worker Despite the Presence of Detectable Neutralizing Antibodies. *Viruses* **2021**, *13*, 661.

(32) Romano, C. M.; Felix, A. C.; Paula, A. V.; Jesus, J. G.; Andrade, P. S.; Candido, D.; Oliveira, F. M.; Ribeiro, A. C.; Silva, F. C. D.; Inemami, M.; Costa, A. A.; Leal, C. O. D.; Figueiredo, W. M.; Pannuti, C. S.; Souza, W. M.; Faria, N. R.; Sabino, E. C. SARS-CoV-2 reinfection caused by the P.1 lineage in Araraquara city, Sao Paulo State, Brazil. *Rev. Inst. Med. Trop. Sao Paulo* **2021**, *63*, No. e36.

(33) da Silva, M. S.; Demoliner, M.; Hansen, A. W.; Gularte, J. S.; Silveira, F.; Heldt, F. H.; Filippi, M.; Pereira, V.; da Silva, F. P.; Mallmann, L.; Fink, P.; da Silva, L. L.; Weber, M. N.; Almeida, P. R.; Fleck, J. D.; Spilki, F. R. Early detection of SARS-CoV-2 P.1 variant in Southern Brazil and reinfection of the same patient by P.2. *Rev. Inst. Med. Trop. Sao Paulo* **2021**, *63*, No. e58.

(34) Zucman, N.; Uhel, F.; Descamps, D.; Roux, D.; Ricard, J. D. Severe reinfection with South African SARS-CoV-2 variant 501Y.V2. *Clin. Infect Dis.* **2021**, *73*, 1945.

(35) Charmet, T.; Schaeffer, L.; Grant, R.; Galmiche, S.; Chény, O.; Von Platen, C.; Maurizot, A.; Rogoff, A.; Omar, F.; David, C.; Septfons, A.; Cauchemez, S.; Gaymard, A.; Lina, B.; Lefrancois, L. H.; Enouf, V.; van der Werf, S.; Mailles, A.; Levy-Bruhl, D.; Carrat, F.; Fontanet, A. Impact of original, B.1.1.7, and B.1.351/P.1 SARS-CoV-2 lineages on vaccine effectiveness of two doses of COVID-19 mRNA vaccines: Results from a nationwide case-control study in France. *Lancet Reg. Health Eur.* **2021**, *8*, 100171.

(36) Imai, M.; Halfmann, P. J.; Yamayoshi, S.; Iwatsuki-Horimoto, K.; Chiba, S.; Watanabe, T.; Nakajima, N.; Ito, M.; Kuroda, M.; Kiso, M.; Maemura, T.; Takahashi, K.; Loeber, S.; Hatta, M.; Koga, M.; Nagai, H.; Yamamoto, S.; Saito, M.; Adachi, E.; Akasaka, O.; Nakamura, M.; Nakachi, I.; Ogura, T.; Baba, R.; Fujita, K.; Ochi, J.; Mitamura, K.; Kato, H.; Nakajima, H.; Yagi, K.; Hattori, S. I.; Maeda, K.; Suzuki, T.; Miyazato, Y.; Valdez, R.; Gherasim, C.; Furusawa, Y.; Okuda, M.; Ujie, M.; Lopes, T. J. S.; Yasuhara, A.; Ueki, H.; Sakai-Tagawa, Y.; Eisfeld, A. J.; Baczenas, J. J.; Baker, D. A.; O'Connor, S. L.; O'Connor, D. H.; Fukushi, S.; Fujimoto, T.; Kuroda, Y.; Gordon, A.; Maeda, K.; Ohmagari, N.; Sugaya, N.; Yotsuyanagi, H.; Mitsuya, H.; Suzuki, T.; Kawaoka, Y. Characterization of a new SARS-CoV-2 variant that emerged in Brazil. *Proc. Natl. Acad. Sci. U. S. A.* **2021**, *118*, No. e2106535118.

(37) Wang, P.; Casner, R. G.; Nair, M. S.; Wang, M.; Yu, J.; Cerutti, G.; Liu, L.; Kwong, P. D.; Huang, Y.; Shapiro, L.; Ho, D. D. Increased resistance of SARS-CoV-2 variant P.1 to antibody neutralization. *Cell Host Microbe* **2021**, *29*, 747−751.e4.

(38) FDA. *Pfizer-BioNTech COVID-19 Vaccine*. Food and Drug Administration 2021. https://www.fda.gov/emergency-preparedness-and-response/coronavirus-disease-2019-covid-19/pfizer-biontech-covid-19-vaccine (accessed 2021 January 26).

(39) FDA. *Moderna COVID-19 Vaccine*. U.S, Food and Drug Administration, 2021. https://www.fda.gov/emergency-preparedness-and-response/coronavirus-disease-2019-covid-19/moderna-covid-19-vaccine (accessed 2021 January 26).

(40) FDA. *FDA Issues Emergency Use Authorization for Third COVID-19 Vaccine*. Food and Drug Administration, 2021. https://www.fda.gov/news-events/press-announcements/fda-issues-emergency-use-authorization-third-covid- (accessed 2021 March 1).

(41) Jackson, L. A.; Anderson, E. J.; Rouphael, N. G.; Roberts, P. C.; Makhene, M.; Coler, R. N.; McCullough, M. P.; Chappell, J. D.; Denison, M. R.; Stevens, L. J.; Pruijssers, A. J.; McDermott, A.; Flach, B.; Doria-Rose, N. A.; Corbett, K. S.; Morabito, K. M.; O'Dell, S.; Schmidt, S. D.; Swanson, P. A., 2nd; Padilla, M.; Mascola, J. R.; Neuzil, K. M.; Bennett, H.; Sun, W.; Peters, E.; Makowski, M.; Albert, J.; Cross, K.; Buchanan, W.; Pikaart-Tautges, R.; Ledgerwood, J. E.; Graham, B. S.; Beigel, J. H.; mRNA-1273 Study Group. An mRNA Vaccine against SARS-CoV-2 - Preliminary Report. *N. Engl. J. Med.* **2020**, *383*, 1920−1931.

(42) Polack, F. P.; Thomas, S. J.; Kitchin, N.; Absalon, J.; Gurtman, A.; Lockhart, S.; Perez, J. L.; Perez Marc, G.; Moreira, E. D.; Zerbini, C.; Bailey, R.; Swanson, K. A.; Roychoudhury, S.; Koury, K.; Li, P.; Kalina, W. V.; Cooper, D.; Frenck, R. W., Jr.; Hammitt, L. L.; Tureci, O.; Nell, H.; Schaefer, A.; Unal, S.; Tresnan, D. B.; Mather, S.; Dormitzer, P. R.; Sahin, U.; Jansen, K. U.; Gruber, W. C.; Clinical Trial Group. Safety and Efficacy of the BNT162b2 mRNA Covid-19 Vaccine. *N .Engl. J. Med.* **2020**, *383*, 2603−2615.

(43) Sadoff, J.; Gray, G.; Vandebosch, A.; Cardenas, V.; Shukarev, G.; Grinsztejn, B.; Goepfert, P. A.; Truyers, C.; Fennema, H.; Spiessens, B.; Offergeld, K.; Scheper, G.; Taylor, K. L.; Robb, M. L.; Treanor, J.; Barouch, D. H.; Stoddard, J.; Ryser, M. F.; Marovich, M. A.; Neuzil, K. M.; Corey, L.; Cauwenberghs, N.; Tanner, T.; Hardt, K.; Ruiz-Guinazu, J.; Le Gars, M.; Schuitemaker, H.; Van Hoof, J.; Struyf, F.; Douoguih, M.; ENSEMBLE Study Group. Safety and Efficacy of Single-Dose Ad26.COV2.S Vaccine against Covid-19. *N. Engl. J. Med.* **2021**, *384*, 2187−2201.

(44) Madhi, S. A.; Baillie, V.; Cutland, C. L.; Voysey, M.; Koen, A. L.; Fairlie, L.; Padayachee, S. D.; Dheda, K.; Barnabas, S. L.; Bhorat, Q. E.; Briner, C.; Kwatra, G.; Ahmed, K.; Aley, P.; Bhikha, S.; Bhiman, J. N.; Bhorat, A. E.; du Plessis, J.; Esmail, A.; Groenewald, M.; Horne, E.; Hwa, S. H.; Jose, A.; Lambe, T.; Laubscher, M.; Malahleha, M.; Masenya, M.; Masilela, M.; McKenzie, S.; Molapo, K.; Moultrie, A.; Oelofse, S.; Patel, F.; Pillay, S.; Rhead, S.; Rodel, H.; Rossouw, L.; Taoushanis, C.; Tegally, H.; Thombrayil, A.; van Eck, S.; Wibmer, C. K.; Durham, N. M.; Kelly, E. J.; Villafana, T. L.; Gilbert, S.; Pollard, A. J.; de Oliveira, T.; Moore, P. L.; Sigal, A.; Izu, A.; NGS-SA Group; Wits-VIDA COVID Group. Efficacy of the ChAdOx1 nCoV-19 Covid-19 Vaccine against the B.1.351 Variant. *N. Engl. J. Med.* **2021**, *384*, 1885−1898.

(45) Shinde, V.; Bhikha, S.; Hoosain, Z.; Archary, M.; Bhorat, Q.; Fairlie, L.; Lalloo, U.; Masilela, M. S. L.; Moodley, D.; Hanley, S.; Fouche, L.; Louw, C.; Tameris, M.; Singh, N.; Goga, A.; Dheda, K.; Grobbelaar, C.; Kruger, G.; Carrim-Ganey, N.; Baillie, V.; de Oliveira, T.; Lombard Koen, A.; Lombaard, J. J.; Mngqibisa, R.; Bhorat, A. E.; Benade, G.; Lalloo, N.; Pitsi, A.; Vollgraaff, P. L.; Luabeya, A.; Esmail, A.; Petrick, F. G.; Oommen-Jose, A.; Foulkes, S.; Ahmed, K.; Thombrayil, A.; Fries, L.; Cloney-Clark, S.; Zhu, M.; Bennett, C.; Albert, G.; Faust, E.; Plested, J. S.; Robertson, A.; Neal, S.; Cho, I.;

https://doi.org/10.1021/acsinfecdis.1c00600
ACS Infect. Dis. XXXX, XXX, XXX−XXX

Glenn, G. M.; Dubovsky, F.; Madhi, S. A.; 2019nCoV-501 Study Group. Efficacy of NVX-CoV2373 Covid-19 Vaccine against the B.1.351 Variant. *N. Engl. J. Med.* **2021**, *384*, 1899−1909.
(46) Jalkanen, P.; Kolehmainen, P.; Häkkinen, H. K.; Huttunen, M.; Tahtinen, P. A.; Lundberg, R.; Maljanen, S.; Reinholm, A.; Tauriainen, S.; Pakkanen, S. H.; Levonen, I.; Nousiainen, A.; Miller, T.; Välimaa, H.; Ivaska, L.; Pasternack, A.; Naves, R.; Ritvos, O.; Österlund, P.; Kuivanen, S.; Smura, T.; Hepojoki, J.; Vapalahti, O.; Lempainen, J.; Kakkola, L.; Kantele, A.; Julkunen, I. COVID-19 mRNA vaccine induced antibody responses against three SARS-CoV-2 variants. *Nat. Commun.* **2021**, *12*, 3991.
(47) Liu, J.; Liu, Y.; Xia, H.; Zou, J.; Weaver, S. C.; Swanson, K. A.; Cai, H.; Cutler, M.; Cooper, D.; Muik, A.; Jansen, K. U.; Sahin, U.; Xie, X.; Dormitzer, P. R.; Shi, P. Y. BNT162b2-elicited neutralization of B.1.617 and other SARS-CoV-2 variants. *Nature* **2021**, *596*, 273−275.
(48) Muik, A.; Wallisch, A. K.; Sänger, B.; Swanson, K. A.; Mühl, J.; Chen, W.; Cai, H.; Maurus, D.; Sarkar, R.; Tureci, O.; Dormitzer, P. R.; Sahin, U. Neutralization of SARS-CoV-2 lineage B.1.1.7 pseudovirus by BNT162b2 vaccine-elicited human sera. *Science* **2021**, *371*, 1152−1153.
(49) Supasa, P.; Zhou, D.; Dejnirattisai, W.; Liu, C.; Mentzer, A. J.; Ginn, H. M.; Zhao, Y.; Duyvesteyn, H. M. E.; Nutalai, R.; Tuekprakhon, A.; Wang, B.; Paesen, G. C.; Slon-Campos, J.; Lopez-Camacho, C.; Hallis, B.; Coombes, N.; Bewley, K. R.; Charlton, S.; Walter, T. S.; Barnes, E.; Dunachie, S. J.; Skelly, D.; Lumley, S. F.; Baker, N.; Shaik, I.; Humphries, H. E.; Godwin, K.; Gent, N.; Sienkiewicz, A.; Dold, C.; Levin, R.; Dong, T.; Pollard, A. J.; Knight, J. C.; Klenerman, P.; Crook, D.; Lambe, T.; Clutterbuck, E.; Bibi, S.; Flaxman, A.; Bittaye, M.; Belij-Rammerstorfer, S.; Gilbert, S.; Hall, D. R.; Williams, M. A.; Paterson, N. G.; James, W.; Carroll, M. W.; Fry, E. E.; Mongkolsapaya, J.; Ren, J.; Stuart, D. I.; Screaton, G. R. Reduced neutralization of SARS-CoV-2 B.1.1.7 variant by convalescent and vaccine sera. *Cell* **2021**, *184*, 2201−2211.e7.
(50) Hilgers, L. A. T.; Blom, A. G. Sucrose fatty acid sulphate esters as novel vaccine adjuvant. *Vaccine* **2006**, *24*, S2-81−S82.
(51) Preston, K. B.; Wong, T. A. S.; To, A.; Tashiro, T. E.; Lieberman, M. M.; Granados, A.; Feliciano, K.; Harrison, J.; Yalley-Ogunro, J.; Elyard, H. A.; Donini, O.; Lehrer, A. T.; Randolph, T. W. Single-vial filovirus glycoprotein vaccines: Biophysical characteristics and immunogenicity after co-lyophilization with adjuvant. *Vaccine* **2021**, *39*, 5650−5657.
(52) Salguero, F. J.; White, A. D.; Slack, G. S.; Fotheringham, S. A.; Bewley, K. R.; Gooch, K. E.; Longet, S.; Humphries, H. E.; Watson, R. J.; Hunter, L.; Ryan, K. A.; Hall, Y.; Sibley, L.; Sarfas, C.; Allen, L.; Aram, M.; Brunt, E.; Brown, P.; Buttigieg, K. R.; Cavell, B. E.; Cobb, R.; Coombes, N. S.; Darby, A.; Daykin-Pont, O.; Elmore, M. J.; Garcia-Dorival, I.; Gkolfinos, K.; Godwin, K. J.; Gouriet, J.; Halkerston, R.; Harris, D. J.; Hender, T.; Ho, C. M. K.; Kennard, C. L.; Knott, D.; Leung, S.; Lucas, V.; Mabbutt, A.; Morrison, A. L.; Nelson, C.; Ngabo, D.; Paterson, J.; Penn, E. J.; Pullan, S.; Taylor, I.; Tipton, T.; Thomas, S.; Tree, J. A.; Turner, C.; Vamos, E.; Wand, N.; Wiblin, N. R.; Charlton, S.; Dong, X.; Hallis, B.; Pearson, G.; Rayner, E. L.; Nicholson, A. G.; Funnell, S. G.; Hiscox, J. A.; Dennis, M. J.; Gleeson, F. V.; Sharpe, S.; Carroll, M. W. Comparison of rhesus and cynomolgus macaques as an infection model for COVID-19. *Nat. Commun.* **2021**, *12*, 1260.
(53) Rockx, B.; Kuiken, T.; Herfst, S.; Bestebroer, T.; Lamers, M. M.; Oude Munnink, B. B.; de Meulder, D.; van Amerongen, G.; van den Brand, J.; Okba, N. M. A.; Schipper, D.; van Run, P.; Leijten, L.; Sikkema, R.; Verschoor, E.; Verstrepen, B.; Bogers, W.; Langermans, J.; Drosten, C.; Fentener van Vlissingen, M.; Fouchier, R.; de Swart, R.; Koopmans, M.; Haagmans, B. L. Comparative pathogenesis of COVID-19, MERS, and SARS in a nonhuman primate model. *Science* **2020**, *368*, 1012−1015.
(54) Lai, C. Y.; To, A.; Wong, T. A. S.; Lieberman, M. M.; Clements, D. E.; Senda, J. T.; Ball, A. H.; Pessaint, L.; Andersen, H.; Furuyama, W.; Marzi, A.; Donini, O.; Lehrer, A. T. Recombinant protein subunit SARS-CoV-2 vaccines formulated with CoVaccine HT adjuvant induce broad, Th1 biased, humoral and cellular immune responses in mice. *Vaccine X* **2021**, 100126.
(55) Baj, A.; Novazzi, F.; Pasciuta, R.; Genoni, A.; Ferrante, F. D.; Valli, M.; Partenope, M.; Tripiciano, R.; Ciserchia, A.; Catanoso, G.; Focosi, D.; Maggi, F. Breakthrough Infections of E484K-Harboring SARS-CoV-2 Delta Variant, Lombardy, Italy. *Emerg. Infect. Dis.* **2021**, *27*, 3180.
(56) Bergwerk, M.; Gonen, T.; Lustig, Y.; Amit, S.; Lipsitch, M.; Cohen, C.; Mandelboim, M.; Levin, E. G.; Rubin, C.; Indenbaum, V.; Tal, I.; Zavitan, M.; Zuckerman, N.; Bar-Chaim, A.; Kreiss, Y.; Regev-Yochay, G. Covid-19 Breakthrough Infections in Vaccinated Health Care Workers. *N. Engl. J. Med.* **2021**, *385*, 1474−1484.
(57) Hacisuleyman, E.; Hale, C.; Saito, Y.; Blachere, N. E.; Bergh, M.; Conlon, E. G.; Schaefer-Babajew, D. J.; DaSilva, J.; Muecksch, F.; Gaebler, C.; Lifton, R.; Nussenzweig, M. C.; Hatziioannou, T.; Bieniasz, P. D.; Darnell, R. B. Vaccine Breakthrough Infections with SARS-CoV-2 Variants. *N. Engl. J. Med.* **2021**, *384*, 2212−2218.
(58) Kroidl, I.; Mecklenburg, I.; Schneiderat, P.; Müller, K.; Girl, P.; Wölfel, R.; Sing, A.; Dangel, A.; Wieser, A.; Hoelscher, M. Vaccine breakthrough infection and onward transmission of SARS-CoV-2 Beta (B.1.351) variant, Bavaria, Germany, February to March 2021. *Euro Surveill* **2021**, *26*, 2100673.
(59) Kustin, T.; Harel, N.; Finkel, U.; Perchik, S.; Harari, S.; Tahor, M.; Caspi, I.; Levy, R.; Leshchinsky, M.; Ken Dror, S.; Bergerzon, G.; Gadban, H.; Gadban, F.; Eliassian, E.; Shimron, O.; Saleh, L.; Ben-Zvi, H.; Keren Taraday, E.; Amichay, D.; Ben-Dor, A.; Sagas, D.; Strauss, M.; Shemer Avni, Y.; Huppert, A.; Kepten, E.; Balicer, R. D.; Netzer, D.; Ben-Shachar, S.; Stern, A. Evidence for increased breakthrough rates of SARS-CoV-2 variants of concern in BNT162b2-mRNA-vaccinated individuals. *Nat. Med.* **2021**, *27*, 1379−1384.
(60) Vignier, N.; Bérot, V.; Bonnave, N.; Peugny, S.; Ballet, M.; Jacoud, E.; Michaud, C.; Gaillet, M.; Djossou, F.; Blanchet, D.; Lavergne, A.; Demar, M.; Nacher, M.; Rousset, D.; Epelboin, L. Breakthrough Infections of SARS-CoV-2 Gamma Variant in Fully Vaccinated Gold Miners, French Guiana, 2021. *Emerg. Infect. Dis.* **2021**, *27*, 2673.
(61) Brown, C. M.; Vostok, J.; Johnson, H.; Burns, M.; Gharpure, R.; Sami, S.; Sabo, R. T.; Hall, N.; Foreman, A.; Schubert, P. L.; Gallagher, G. R.; Fink, T.; Madoff, L. C.; Gabriel, S. B.; MacInnis, B.; Park, D. J.; Siddle, K. J.; Harik, V.; Arvidson, D.; Brock-Fisher, T.; Dunn, M.; Kearns, A.; Laney, A. S. Outbreak of SARS-CoV-2 Infections, Including COVID-19 Vaccine Breakthrough Infections, Associated with Large Public Gatherings - Barnstable County, Massachusetts, July 2021. *Morb. Mortal. Wkly. Rep.* **2021**, *70*, 1059−1062.
(62) Corbett, K. S.; Werner, A. P.; O'Connell, S.; Gagne, M.; Lai, L.; Moliva, J. I.; Flynn, B.; Choi, A.; Koch, M.; Foulds, K. E.; Andrew, S. F.; Flebbe, D. R.; Lamb, E.; Nurmukhambetova, S. T.; Provost, S. J.; Bock, K. W.; Minai, M.; Nagata, B. M.; Ry, A. V.; Flinchbaugh, Z.; Johnston, T. S.; Mokhtari, E. B.; Mudvari, P.; Henry, A. R.; Laboune, F.; Chang, B.; Porto, M.; Wear, J.; Alvarado, G. S.; Boyoglu-Barnum, S.; Todd, J. M.; Bart, B.; Cook, A.; Dodson, A.; Pessaint, L.; Steingrebe, K.; Elbashir, S.; Sriparna, M.; Pekosz, A.; Andersen, H.; Wu, K.; Edwards, D. K.; Kar, S.; Lewis, M. G.; Boritz, E.; Moore, I. N.; Carfi, A.; Suthar, M. S.; McDermott, A.; Roederer, M.; Nason, M. C.; Sullivan, N. J.; Douek, D. C.; Graham, B. S.; Seder, R. A. mRNA-1273 protects against SARS-CoV-2 beta infection in nonhuman primates. *Nat. Immunol.* **2021**, *22*, 1306−1315.
(63) Pegu, A.; O'Connell, S. E.; Schmidt, S. D.; O'Dell, S.; Talana, C. A.; Lai, L.; Albert, J.; Anderson, E.; Bennett, H.; Corbett, K. S.; Flach, B.; Jackson, L.; Leav, B.; Ledgerwood, J. E.; Luke, C. J.; Makowski, M.; Nason, M. C.; Roberts, P. C.; Roederer, M.; Rebolledo, P. A.; Rostad, C. A.; Rouphael, N. G.; Shi, W.; Wang, L.; Widge, A. T.; Yang, E. S.; The MRNA-1273 Study Group; Beigel, J. H.; Graham, B. S.; Mascola, J. R.; Suthar, M. S.; McDermott, A. B.; Doria-Rose, N. A. Durability of mRNA-1273 vaccine-induced antibodies against SARS-CoV-2 variants. *Science* **2021**, *373*, 1372−1377.

https://doi.org/10.1021/acsinfecdis.1c00600
ACS Infect. Dis. XXXX, XXX, XXX−XXX

(64) Yu, J.; Tostanoski, L. H.; Mercado, N. B.; McMahan, K.; Liu, J.; Jacob-Dolan, C.; Chandrashekar, A.; Atyeo, C.; Martinez, D. R.; Anioke, T.; Bondzie, E. A.; Chang, A.; Gardner, S.; Giffin, V. M.; Hope, D. L.; Nampanya, F.; Nkolola, J.; Patel, S.; Sanborn, O.; Sellers, D.; Wan, H.; Hayes, T.; Bauer, K.; Pessaint, L.; Valentin, D.; Flinchbaugh, Z.; Brown, R.; Cook, A.; Bueno-Wilkerson, D.; Teow, E.; Andersen, H.; Lewis, M. G.; Martinot, A. J.; Baric, R. S.; Alter, G.; Wegmann, F.; Zahn, R.; Schuitemaker, H.; Barouch, D. H. Protective efficacy of Ad26.COV2.S against SARS-CoV-2 B.1.351 in macaques. *Nature* **2021**, *596*, 423−427.

(65) Choi, A.; Koch, M.; Wu, K.; Dixon, G.; Oestreicher, J.; Legault, H.; Stewart-Jones, G. B. E.; Colpitts, T.; Pajon, R.; Bennett, H.; Carfi, A.; Edwards, D. K. Serum Neutralizing Activity of mRNA-1273 against SARS-CoV-2 Variants. *J. Virol.* **2021**, *95*, No. e0131321.

(66) Wu, K.; Werner, A. P.; Koch, M.; Choi, A.; Narayanan, E.; Stewart-Jones, G. B. E.; Colpitts, T.; Bennett, H.; Boyoglu-Barnum, S.; Shi, W.; Moliva, J. I.; Sullivan, N. J.; Graham, B. S.; Carfi, A.; Corbett, K. S.; Seder, R. A.; Edwards, D. K. Serum Neutralizing Activity Elicited by mRNA-1273 Vaccine. *N. Engl. J. Med.* **2021**, *384*, 1468−1470.

(67) Lucas, C.; Vogels, C. B. F.; Yildirim, I.; Rothman, J. E.; Lu, P.; Monteiro, V.; Gehlhausen, J. R.; Campbell, M.; Silva, J.; Tabachnikova, A.; Peña-Hernandez, M. A.; Muenker, M. C.; Breban, M. I.; Fauver, J. R.; Mohanty, S.; Huang, J.; Yale, S.-C.-G. S. I.; Shaw, A. C.; Ko, A. I.; Omer, S. B.; Grubaugh, N. D.; Iwasaki, A. Impact of circulating SARS-CoV-2 variants on mRNA vaccine-induced immunity. *Nature* **2021**, *600*, 523−529.

(68) Fahlberg, M. D.; Blair, R. V.; Doyle-Meyers, L. A.; Midkiff, C. C.; Zenere, G.; Russell-Lodrigue, K. E.; Monjure, C. J.; Haupt, E. H.; Penney, T. P.; Lehmicke, G.; Threeton, B. M.; Golden, N.; Datta, P. K.; Roy, C. J.; Bohm, R. P.; Maness, N. J.; Fischer, T.; Rappaport, J.; Vaccari, M. Cellular events of acute, resolving or progressive COVID-19 in SARS-CoV-2 infected non-human primates. *Nat. Commun.* **2020**, *11*, 6078.

(69) Guebre-Xabier, M.; Patel, N.; Tian, J. H.; Zhou, B.; Maciejewski, S.; Lam, K.; Portnoff, A. D.; Massare, M. J.; Frieman, M. B.; Piedra, P. A.; Ellingsworth, L.; Glenn, G.; Smith, G. NVX-CoV2373 vaccine protects cynomolgus macaque upper and lower airways against SARS-CoV-2 challenge. *Vaccine* **2020**, *38*, 7892−7896.

(70) Woolsey, C.; Borisevich, V.; Prasad, A. N.; Agans, K. N.; Deer, D. J.; Dobias, N. S.; Heymann, J. C.; Foster, S. L.; Levine, C. B.; Medina, L.; Melody, K.; Geisbert, J. B.; Fenton, K. A.; Geisbert, T. W.; Cross, R. W. Establishment of an African green monkey model for COVID-19 and protection against re-infection. *Nat. Immunol.* **2021**, *22*, 86−98.

(71) Malladi, S. K.; Patel, U. R.; Rajmani, R. S.; Singh, R.; Pandey, S.; Kumar, S.; Khaleeq, S.; van Vuren, P. J.; Riddell, S.; Goldie, S.; Gayathri, S.; Chakraborty, D.; Kalita, P.; Pramanick, I.; Agarwal, N.; Reddy, P.; Girish, N.; Upadhyaya, A.; Khan, M. S.; Kanjo, K.; Bhat, M.; Mani, S.; Bhattacharyya, S.; Siddiqui, S.; Tyagi, A.; Jha, S.; Pandey, R.; Tripathi, S.; Dutta, S.; McAuley, A. J.; Singanallur, N. B.; Vasan, S. S.; Ringe, R. P.; Varadarajan, R. Immunogenicity and Protective Efficacy of a Highly Thermotolerant, Trimeric SARS-CoV-2 Receptor Binding Domain Derivative. *ACS Infect. Dis.* **2021**, *7*, 2546−2564.

(72) Ellis, D.; Brunette, N.; Crawford, K. H. D.; Walls, A. C.; Pham, M. N.; Chen, C.; Herpoldt, K. L.; Fiala, B.; Murphy, M.; Pettie, D.; Kraft, J. C.; Malone, K. D.; Navarro, M. J.; Ogohara, C.; Kepl, E.; Ravichandran, R.; Sydeman, C.; Ahlrichs, M.; Johnson, M.; Blackstone, A.; Carter, L.; Starr, T. N.; Greaney, A. J.; Lee, K. K.; Veesler, D.; Bloom, J. D.; King, N. P. Stabilization of the SARS-CoV-2 Spike Receptor-Binding Domain Using Deep Mutational Scanning and Structure-Based Design. *Front. Immunol.* **2021**, *12*, 710263.

(73) Mabrouk, M. T.; Chiem, K.; Rujas, E.; Huang, W. C.; Jahagirdar, D.; Quinn, B.; Surendran Nair, M.; Nissly, R. H.; Cavener, V. S.; Boyle, N. R.; Sornberger, T. A.; Kuchipudi, S. V.; Ortega, J.; Julien, J. P.; Martinez-Sobrido, L.; Lovell, J. Lyophilized, thermostable Spike or RBD immunogenic liposomes induce protective immunity against SARS-CoV-2 in mice. *Sci. Adv.* **2021**, *7*, No. eabj1476.

(74) Chmielewska, A. M.; Naddeo, M.; Capone, S.; Ammendola, V.; Hu, K.; Meredith, L.; Verhoye, L.; Rychlowska, M.; Rappuoli, R.; Ulmer, J. B.; Colloca, S.; Nicosia, A.; Cortese, R.; Leroux-Roels, G.; Balfe, P.; Bienkowska-Szewczyk, K.; Meuleman, P.; McKeating, J. A.; Folgori, A. Combined adenovirus vector and hepatitis C virus envelope protein prime-boost regimen elicits T cell and neutralizing antibody immune responses. *J. Virol.* **2014**, *88*, 5502−5510.

(75) Choi, J. A.; Goo, J.; Yang, E.; Jung, D. I.; Lee, S.; Rho, S.; Jeong, Y.; Park, Y. S.; Park, H.; Moon, Y. H.; Park, U.; Seo, S. H.; Lee, H.; Lee, J. M.; Cho, N. H.; Song, M.; Kim, J. O. Cross-Protection against MERS-CoV by Prime-Boost Vaccination Using Viral Spike DNA and Protein. *J. Virol.* **2020**, *94*, No. e01176.

(76) Gilbert, S. C.; Lambe, T. Recombinant protein vaccines against SARS-CoV-2. *Lancet Infect. Dis.* **2021**, *21*, 1337−1338.

(77) Mandolesi, M.; Sheward, D. J.; Hanke, L.; Ma, J.; Pushparaj, P.; Perez Vidakovics, L.; Kim, C.; Àdori, M.; Lenart, K.; Loré, K.; Castro Dopico, X.; Coquet, J. M.; McInerney, G. M.; Karlsson Hedestam, G. B.; Murrell, B. SARS-CoV-2 protein subunit vaccination of mice and rhesus macaques elicits potent and durable neutralizing antibody responses. *Cell Rep. Med.* **2021**, *2*, 100252.

(78) Goepfert, P. A.; Fu, B.; Chabanon, A. L.; Bonaparte, M. I.; Davis, M. G.; Essink, B. J.; Frank, I.; Haney, O.; Janosczyk, H.; Keefer, M. C.; Koutsoukos, M.; Kimmel, M. A.; Masotti, R.; Savarino, S. J.; Schuerman, L.; Schwartz, H.; Sher, L. D.; Smith, J.; Tavares-Da-Silva, F.; Gurunathan, S.; DiazGranados, C. A.; de Bruyn, G. Safety and immunogenicity of SARS-CoV-2 recombinant protein vaccine formulations in healthy adults: interim results of a randomised, placebo-controlled, phase 1-2, dose-ranging study. *Lancet Infect. Dis.* **2021**, *21*, 1257−1270.

(79) Alter, G.; Yu, J.; Liu, J.; Chandrashekar, A.; Borducchi, E. N.; Tostanoski, L. H.; McMahan, K.; Jacob-Dolan, C.; Martinez, D. R.; Chang, A.; Anioke, T.; Lifton, M.; Nkolola, J.; Stephenson, K. E.; Atyeo, C.; Shin, S.; Fields, P.; Kaplan, I.; Robins, H.; Amanat, F.; Krammer, F.; Baric, R. S.; Le Gars, M.; Sadoff, J.; de Groot, A. M.; Heerwegh, D.; Struyf, F.; Douoguih, M.; van Hoof, J.; Schuitemaker, H.; Barouch, D. H. Immunogenicity of Ad26.COV2.S vaccine against SARS-CoV-2 variants in humans. *Nature* **2021**, *596*, 268−272.

(80) Joyce, M. G.; King, H. A. D.; Elakhal-Naouar, I.; Ahmed, A.; Peachman, K. K.; Macedo Cincotta, C.; Subra, C.; Chen, R. E.; Thomas, P. V.; Chen, W. H.; Sankhala, R. S.; Hajduczki, A.; Martinez, E. J.; Peterson, C. E.; Chang, W. C.; Choe, M.; Smith, C.; Lee, P. J.; Headley, J. A.; Taddese, M. G.; Elyard, H. A.; Cook, A.; Anderson, A.; Wuertz, K. M.; Dong, M.; Swafford, I.; Case, J. B.; Currier, J. R.; Lal, K. G.; Molnar, S.; Nair, M. S.; Dussupt, V.; Daye, S. P.; Zeng, X.; Barkei, E. K.; Staples, H. M.; Alfson, K.; Carrion, R.; Krebs, S. J.; Paquin-Proulx, D.; Karasavva, N.; Polonis, V. R.; Jagodzinski, L. L.; Amare, M. F.; Vasan, S.; Scott, P. T.; Huang, Y.; Ho, D. D.; de Val, N.; Diamond, M. S.; Lewis, M. G.; Rao, M.; Matyas, G. R.; Gromowski, G. D.; Peel, S. A.; Michael, N. L.; Bolton, D. L.; Modjarrad, K. A SARS-CoV-2 ferritin nanoparticle vaccine elicits protective immune responses in nonhuman primates. *Sci. Transl. Med.* **2022**, No. eabi5735.

(81) Purushotham, J. N.; van Doremalen, N.; Munster, V. J. SARS-CoV-2 vaccines: anamnestic response in previously infected recipients. *Cell Res.* **2021**, *31*, 827−828.

(82) Sprenger, K. G.; Louveau, J. E.; Murugan, P. M.; Chakraborty, A. K. Optimizing immunization protocols to elicit broadly neutralizing antibodies. *Proc. Natl. Acad. Sci. U. S. A.* **2020**, *117*, 20077−20087.

(83) Salzberger, B.; Buder, F.; Lampl, B.; Ehrenstein, B.; Hitzenbichler, F.; Holzmann, T.; Schmidt, B.; Hanses, F. Epidemiology of SARS-CoV-2. *Infection* **2021**, *49*, 233−239.

(84) Widge, A. T.; Rouphael, N. G.; Jackson, L. A.; Anderson, E. J.; Roberts, P. C.; Makhene, M.; Chappell, J. D.; Denison, M. R.; Stevens, L. J.; Pruijssers, A. J.; McDermott, A. B.; Flach, B.; Lin, B. C.; Doria-Rose, N. A.; O'Dell, S.; Schmidt, S. D.; Neuzil, K. M.; Bennett, H.; Leav, B.; Makowski, M.; Albert, J.; Cross, K.; Edara, V. V.; Floyd, K.; Suthar, M. S.; Buchanan, W.; Luke, C. J.; Ledgerwood, J. E.; Mascola, J. R.; Graham, B. S.; Beigel, J. H.; mRNA-1273 Study Group.

https://doi.org/10.1021/acsinfecdis.1c00600
ACS Infect. Dis. XXXX, XXX, XXX−XXX

Durability of Responses after SARS-CoV-2 mRNA-1273 Vaccination. *N. Engl. J. Med.* **2021**, *384*, 80−82.
(85) Barouch, D. H.; Stephenson, K. E.; Sadoff, J.; Yu, J.; Chang, A.; Gebre, M.; McMahan, K.; Liu, J.; Chandrashekar, A.; Patel, S.; Le Gars, M.; de Groot, A. M.; Heerwegh, D.; Struyf, F.; Douoguih, M.; van Hoof, J.; Schuitemaker, H. Durable Humoral and Cellular Immune Responses 8 Months after Ad26. COV2.S Vaccination. *N. Engl. J. Med.* **2021**, *385*, 951−953.
(86) Goel, R. R.; Painter, M. M.; Apostolidis, S. A.; Mathew, D.; Meng, W.; Rosenfeld, A. M.; Lundgreen, K. A.; Reynaldi, A.; Khoury, D. S.; Pattekar, A.; Gouma, S.; Kuri-Cervantes, L.; Hicks, P.; Dysinger, S.; Hicks, A.; Sharma, H.; Herring, S.; Korte, S.; Baxter, A. E.; Oldridge, D. A.; Giles, J. R.; Weirick, M. E.; McAllister, C. M.; Awofolaju, M.; Tanenbaum, N.; Drapeau, E. M.; Dougherty, J.; Long, S.; D'Andrea, K.; Hamilton, J. T.; McLaughlin, M.; Williams, J. C.; Adamski, S.; Kuthuru, O.; The Upenn Covid Processing Unit; Frank, I.; Betts, M. R.; Vella, L. A.; Grifoni, A.; Weiskopf, D.; Sette, A.; Hensley, S. E.; Davenport, M. P.; Bates, P.; Luning Prak, E. T.; Greenplate, A. R.; Wherry, E. J. mRNA vaccines induce durable immune memory to SARS-CoV-2 and variants of concern. *Science* **2021**, *374*, No. abm0829.
(87) Blachere, N. E.; Hacisuleyman, E.; Darnell, R. B. Vaccine Breakthrough Infections with SARS-CoV-2 Variants. *Reply*. *N. Engl. J. Med.* **2021**, *385*, No. e7.
(88) Cheng, S. M. S.; Mok, C. K. P.; Leung, Y. W. Y.; Ng, S. S.; Chan, K. C. K.; Ko, F. W.; Chen, C.; Yiu, K.; Lam, B. H. S.; Lau, E. H. Y.; Chan, K. K. P.; Luk, L. L. H.; Li, J. K. C.; Tsang, L. C. H.; Poon, L. L. M.; Hui, D. S. C.; Peiris, M. Neutralizing antibodies against the SARS-CoV-2 Omicron variant following homologous and heterologous CoronaVac or BNT162b2 vaccination. *Nat. Med.* **2022**, DOI: 10.1038/s41591-022-01704-7.
(89) Gruell, H.; Vanshylla, K.; Tober-Lau, P.; Hillus, D.; Schommers, P.; Lehmann, C.; Kurth, F.; Sander, L. E.; Klein, F. mRNA booster immunization elicits potent neutralizing serum activity against the SARS-CoV-2 Omicron variant. *Nat. Med.* **2022**, DOI: 10.1038/s41591-021-01676-0.
(90) Liu, L.; Iketani, S.; Guo, Y.; Chan, J. F.-W.; Wang, M.; Liu, L.; Luo, Y.; Chu, H.; Huang, Y.; Nair, M. S.; Yu, J.; Chik, K. K.-H.; Yuen, T. T.-T.; Yoon, C.; To, K. K.; Chen, H.; Yin, M. T.; Sobieszczyk, M. E.; Huang, Y.; Wang, H. H.; Sheng, Z.; Yuen, K. Y.; Ho, D. D. Striking Antibody Evasion Manifested by the Omicron Variant of SARS-CoV-2. *Nature* **2022**, 676.
(91) Carreno, J. M.; Alshammary, H.; Tcheou, J.; Singh, G.; Raskin, A.; Kawabata, H.; Sominsky, L.; Clark, J.; Adelsberg, D. C.; Bielak, D.; Gonzalez-Reiche, A. S.; Dambrauskas, N.; Vigdorovich, V.; Group, P. P. S.; Srivastava, K.; Sather, D. N.; Sordillo, E. M.; Bajic, G.; van Bakel, H.; Simon, V.; Krammer, F. Activity of convalescent and vaccine serum against SARS-CoV-2 Omicron. *Nature* **2022**, 682.
(92) Dejnirattisai, W.; Shaw, R. H.; Supasa, P.; Liu, C.; Stuart, A. S.; Pollard, A. J.; Liu, X.; Lambe, T.; Crook, D.; Stuart, D. I.; Mongkolsapaya, J.; Nguyen-Van-Tam, J. S.; Snape, M. D.; Screaton, G. R. Reduced neutralisation of SARS-CoV-2 omicron B.1.1.529 variant by post-immunisation serum. *Lancet* **2022**, *399*, 234−236.
(93) To, A.; Medina, L. O.; Mfuh, K. O.; Lieberman, M. M.; Wong, T. A. S.; Namekar, M.; Nakano, E.; Lai, C. Y.; Kumar, M.; Nerurkar, V. R.; Lehrer, A. T. Recombinant Zika Virus Subunits Are Immunogenic and Efficacious in Mice. *mSphere* **2018**, *3*, No. e00576.
(94) Namekar, M.; Kumar, M.; O'Connell, M.; Nerurkar, V. R. Effect of serum heat-inactivation and dilution on detection of anti-WNV antibodies in mice by West Nile virus E-protein microsphere immunoassay. *PLoS One* **2012**, *7*, No. e45851.
(95) Haun, B. K.; Lai, C. Y.; Williams, C. A.; Wong, T. A. S.; Lieberman, M. M.; Pessaint, L.; Andersen, H.; Lehrer, A. T. CoVaccine HT Adjuvant Potentiates Robust Immune Responses to Recombinant SARS-CoV-2 Spike S1 Immunization. *Front. Immunol.* **2020**, *11*, 599587.
(96) Furuyama, W.; Shifflett, K.; Pinski, A. N.; Griffin, A. J.; Feldmann, F.; Okumura, A.; Gourdine, T.; Jankeel, A.; Lovaglio, J.; Hanley, P. W.; Thomas, T.; Clancy, C. S.; Messaoudi, I.; O'Donnell, K. L.; Marzi, A. Rapid Protection from COVID-19 in Nonhuman Primates Vaccinated Intramuscularly but Not Intranasally with a Single Dose of a Vesicular Stomatitis Virus-Based Vaccine. *MBio* **2022**, No. e0337921.
(97) Reed, L. J.; Muench, H. A simple method of estimating fifty percent end points. *Am. J. Epidemiol.* **1938**, *27*, 493−497.

https://doi.org/10.1021/acsinfecdis.1c00600
ACS Infect. Dis. XXXX, XXX, XXX−XXX